

Quantum Algorithms for Nonlinear Differential Equations via Pivot-Shifted Carleman Linearization

Ke Wang,^{*} Zikang Jia,^{*} Shravan Veerapaneni, and Zhiyan Ding[†]

Department of Mathematics, University of Michigan

We develop a pivot-shifted Carleman linearization framework for quantum algorithms solving quadratic nonlinear ordinary differential equations. By shifting the dynamics by a pivot state prior to Carleman lifting, and combining this with a Lyapunov transform and rescaling, we enlarge the class of nonlinear systems that can be efficiently simulated on quantum computers. For systems that exhibit stability in the shifted coordinates, we establish long time convergence of the truncated Carleman embedding. We prove that the truncation order scales only logarithmically with the simulation time and target precision, and we derive end-to-end quantum query complexity bounds for preparing a state proportional to the final solution. By introducing a modified nonlinearity condition, this framework entirely removes the conventional lower bound requirement on the initial condition. For more general systems that remain unstable after shifting, we provide short time convergence guarantees that are similarly free from the initial condition constraints. Numerical experiments on the logistic and the Lotka–Volterra equations demonstrate that an appropriate pivot choice improves stability and accuracy, and yields exponential error decay with truncation order. These results show that pivot shifting provides a practical and theoretically justified route for extending Carleman-based quantum algorithms to a broader class of nonlinear dynamical systems.

I. INTRODUCTION

Over the past several decades, quantum algorithms have attracted sustained interest because of their potential to provide significant speedups over classical methods [1]. One of the most important quantum algorithmic primitives is the simulation of quantum systems, where the curse of dimensionality arises naturally and severely limits classical approaches. Since quantum dynamics are themselves governed by quantum mechanics, they are especially well suited for implementation on quantum computers. This structural compatibility has led to remarkable advances, including optimal-scaling Hamiltonian simulation [2, 3] and near-optimal-scaling Lindblad simulation [4–6]. Building on these developments, recent works have begun to explore quantum advantages for more general classical computational tasks [7, 8], including linear system solvers [9, 10] and algorithms for linear differential equations [11–17], largely by exploiting the intrinsic linearity of quantum mechanics.

Although quantum computing offers powerful tools for simulating linear systems, many phenomena of scientific and practical interest are governed by nonlinear differential equations, including models arising in plasma physics, engineering, economics, and chemical reactions [18–21]. Their nonlinear structure makes accurate simulation substantially more challenging, even on modern classical high-performance computing platforms. The difficulty is even more fundamental on a quantum computer: the evolution generated by quantum mechanics is intrinsically linear, whereas the target dynamics are nonlinear. Therefore, a quantum algorithm cannot usually implement the nonlinear flow directly, and must instead represent it through an auxiliary linear framework or through intermediate operations that effectively reproduce the nonlinear behavior. This basic mismatch between linear quantum evolution and nonlinear target dynamics is the central obstacle in designing quantum algorithms for nonlinear differential equations.

Existing quantum approaches to nonlinear differential equations can largely be viewed as different strategies for overcoming the basic mismatch between linear quantum evolution and nonlinear target dynamics. The Koopman–von Neumann framework embeds the dynamics into a linear operator evolution acting on observables or functions of the state, rather than directly on the state itself [22]. Variational and hybrid quantum-classical methods offer a near term pathway by recasting nonlinear dynamics as optimization problems using parameterized quantum circuits, although the rigorous error analyses are not fully established [23, 24]. Other early approaches similarly relied on more general linearization or approximation schemes to indirectly mimic nonlinear evolution on a quantum computer [25]. Among these methods, Carleman linearization has emerged as one of the most promising frameworks. Its central idea is to lift the nonlinear system into a higher dimensional linear system by enlarging the state space and encoding higher order monomials of the solution [26–28]. This construction is particularly attractive because it is systematic, compatible

^{*} These authors contributed equally to this work.

[†] zyding@umich.edu

with quantum linear system techniques, and admits rigorous error analysis. Under dissipativity assumptions and a condition analogous to the Reynolds number in fluid dynamics, it yields efficient quantum simulation algorithms that remain stable for a long time [26]. Extensions beyond the dissipative regime have also been established for nonresonant systems [29], as well as for stable and conservative systems [27].

Despite this progress, the current applicability of Carleman linearization still relies on rather restrictive assumptions. These assumptions not only narrow the class of nonlinear systems that can be treated efficiently, but also impose nontrivial conditions on the initial value in order to guarantee convergence of the truncated Carleman expansion. Specifically, consider the n -dimensional quadratic ordinary differential equation

$$\partial_t x = F_2 x^{\otimes 2} + F_1 x + F_0, \quad x(0) = x_0, \quad (1)$$

where $x \in \mathbb{R}^n$, $x^{\otimes 2} \in \mathbb{R}^{n^2}$, $F_2 \in \mathbb{R}^{n \times n^2}$, $F_1 \in \mathbb{R}^{n \times n}$, and $F_0 \in \mathbb{R}^n$. Existing analyses [26–28] typically establish efficient quantum algorithms under three primary conditions. First, the linear part is required to be dissipative, meaning its spectral abscissa satisfies $\alpha(F_1) < 0$. Second, a constraint similar to the Reynolds number is imposed,

$$R := \frac{1}{-\alpha(F_1)} \left(\|x(0)\| \|F_2\| + \frac{\|F_0\|}{\|x(0)\|} \right) < 1. \quad (2)$$

This condition ensures that the dissipative effect of the linear term dominates both the nonlinear term and the forcing term, so that the norm of the solution remains nonincreasing. Furthermore, because R scales inversely with the initial norm, $1/\|x(0)\|$, one needs a third condition, $\delta \leq \|x(0)\| \leq 1$ for some fixed $\delta > 0$.

Although these conditions are sufficient to guarantee efficient quantum algorithms, they are quite restrictive and describe a much narrower regime than the full class of nonlinear systems that are stable in the usual dynamical-systems sense. Many stable systems of practical interest fall outside this framework, and for such systems, establishing an end-to-end quantum advantage becomes substantially more challenging [8]. A simple example is the logistic equation $\partial_t x = x - x^2$. For every initial condition $x(0) > 0$, the solution remains bounded and converges to a stable equilibrium. However, the linear coefficient is positive, and hence the condition $\alpha(F_1) < 0$ fails. In this case, the standard Carleman approximation can diverge on long time scales and fail to achieve high accuracy, as demonstrated by our numerical experiments in Section V. Nevertheless, the underlying nonlinear dynamics are stable. It is therefore natural to ask whether one can develop provably efficient quantum algorithms that capture the dynamics of such systems. More generally, given the limitations of existing Carleman-based criteria, one may ask whether provably efficient quantum algorithms can be developed under weaker assumptions than those currently required. This leads to the first central question of our work:

Can we develop provably efficient algorithms under weaker stable assumptions?

Beyond stable nonlinear systems, many systems of practical interest are unstable, and it is important to understand the scope of quantum algorithms in this broader setting. For unstable systems, solutions may grow rapidly, often exponentially in time, so one generally expects efficient simulation to be possible only over finite or short time intervals. However, since the convergence guarantees for existing Carleman linearization methods rely strongly on stability assumptions and restrictions on the initial condition, the method fails to converge even on short time intervals for a large class of unstable systems, and hence fail to capture the dynamics with high accuracy. On the other hand, the solution of an unstable nonlinear system may still be well approximated by a linearized or lifted linear system over sufficiently short time intervals. It is therefore natural to ask whether Carleman linearization can be modified to capture this behavior on short time scales while still retaining rigorous convergence guarantees. This leads to the second central question of our work:

How can we capture the dynamics of unstable systems at least for short time scales with rigorous convergence guarantees?

In this work, we provide a modified Carleman linearization framework that addresses both questions above. Inspired by the classical idea of pivot rule in linear programming [30, 31], we introduce a pivot-shifted Carleman linearization method. The main idea is to shift the dynamics by a pivot state s and apply Carleman linearization to the shifted variable $u = x - s$, rather than directly to the original variable x . This produces a transformed quadratic system whose linear part can be substantially better behaved than that of the original equation.

We rigorously demonstrate that this modification significantly broadens the regime in which Carleman-based quantum algorithms can be analyzed. With a suitable choice of pivot, we establish long time convergence guarantees under assumptions that are strictly weaker and more flexible than the standard Carleman criteria. In particular, for a stable system that does not satisfy $\alpha(F_1) < 0$, the pivot-shifted Carleman linearization can still yield an efficient quantum algorithm, provided that the pivot is chosen appropriately. The method remains useful even when the shifted system

is still unstable. In this case, we prove short time convergence guarantees and show that pivot shifting can weaken the dependence on the initial condition while extending the time interval over which the Carleman approximation remains accurate.

Taken together, our results show both theoretically and numerically that pivot shifting plays two complementary roles. For stable systems, it enlarges the class of problems that admit efficient long time simulation. For unstable systems, it improves the effective short time approximation regime and allows the dynamics to be captured over longer time scales than standard Carleman linearization permits.

A. Main results

Our main results are obtained through a pivot-shifted Carleman linearization of the quadratic ordinary differential equation in Eq. (1). For a chosen pivot s , we introduce the shifted variable $u = x - s$, which satisfies

$$\partial_t u = F_{2,s} u^{\otimes 2} + F_{1,s} u + F_{0,s}. \quad (3)$$

We then apply a Lyapunov transformation together with a rescaling by setting $v = Qu$, where Q is chosen to control the stability and magnitude of the shifted dynamics. Carleman lifting is then applied to the transformed variable v . This pivot shifted formulation allows us to reduce the effective initial displacement and enforce a dissipativity condition on the transformed linear part.

We say that the differential equation becomes stable after pivot shifting if the following assumption holds:

Assumption I.1 (Stability after pivot shift). *The spectral abscissa of $F_{1,s}$ is negative, namely*

$$\alpha(F_{1,s}) = \max_i \operatorname{Re}(\lambda_i(F_{1,s})) < 0. \quad (4)$$

By the Lyapunov theorem, Assumption I.1 implies that there exists a positive definite matrix $P \succ 0$ such that

$$PF_{1,s} + F_{1,s}^\dagger P \prec 0. \quad (5)$$

It reveals that the shifted linear dynamics is dissipative in the weighted inner product induced by P . Using the corresponding weighted norm $\|\cdot\|_P$ and logarithmic norm $\mu_P(\cdot)$, we impose the following condition.

Assumption I.2 (Weighted nonlinear stability condition). $\mu_P(F_{1,s})^2 - 4\|F_{2,s}\|_P\|F_{0,s}\|_P > 0$.

This condition plays a role analogous to the requirement $R < 1$ in [26, 27]. Unlike the Reynolds-number-type condition in Eq. (2), this assumption does not place the initial state $u(0)$ in the denominator, and therefore avoids the singular behavior caused by the absence of a positive lower bound on the initial value.

Assumption I.1, together with the choice of the Lyapunov matrix P , makes the shifted linear dynamics strictly dissipative in the P weighted norm, $\mu_P(F_{1,s}) < 0$. Assumption I.2 controls the nonlinearity contribution by ensuring that the corresponding quadratic inequality has two distinct positive roots. These assumptions together identify a regime in which the pivot-shifted Carleman system inherits a dissipativity structure in the transformed coordinates. It is worth noting that the efficient implementation of the shifted Carleman linearization requires an efficient transformation between the original variable x and the shifted variable $u = x - s$. This issue is discussed mainly in Section II. In this work, the computational cost of the algorithm is stated under the same cost model as in [26, 27]. Specifically, our complexity estimates assume an input model in which we have access to block encodings of F_2 , F_1 , F_0 , and Q , state preparation oracles for $|x(0)\rangle$ and $|s\rangle$, and the values of $\|x(0)\|$ and $\|s\|$.

We first state the main result for stable shifted systems, which establishes long time convergence of the pivot-shifted Carleman linearization and provides the corresponding quantum query complexity:

Theorem I.3 (Informal complexity for stable shifted systems). *Suppose Assumptions I.1 and I.2 hold. Let $Q = \sqrt{P}/\gamma$ for a suitable rescaling parameter $\gamma > 0$, and let $v = Q(x - s)$ be the transformed shifted variable. Then there exists a quantum algorithm that outputs an ϵ -approximation of the final state $|x(T)\rangle$ using*

$$\tilde{\mathcal{O}} \left(\frac{\sqrt{\|x(T) - s\|^2 + \|s\|^2}}{\|x(T)\|} \frac{\sqrt{\|x(0)\|^2 + \|s\|^2}}{\|x(0) - s\|} \frac{\max_{t \in [0, T]} \|v(t)\|}{\|v(T)\|} \sqrt{T} \operatorname{poly} \log(1/\epsilon) \right) \quad (6)$$

queries to the block encodings of Q and F_i , and to the state-preparation oracles for $|x(0)\rangle$ and $|s\rangle$. Here, $\tilde{\mathcal{O}}(\cdot)$ suppresses logarithmic factors and constants associated with the block encoding normalizations and condition parameters of the transformed system.

Remark I.4. *The choice of the pivot s in the stable case is crucial for the efficiency of the quantum algorithm. In particular, s should be chosen such that $F_{2,s}, F_{1,s}, F_{0,s}$ satisfies the stable condition in Assumption I.1. The ideal choice of s depends on the specific system and may require some prior knowledge of the dynamics. One useful guideline is to choose s to be a stable equilibrium of the system, if such an equilibrium exists. For example, if the system has a locally exponentially stable equilibrium x^* , then $F_{1,x^*} := F_1 + F_2(x^* \otimes I_n + I_n \otimes x^*)$ has a negative spectral abscissa, meaning Assumption I.1 is satisfied with $s = x^*$. In addition, $F_{0,x^*} = F_0 + F_1 x^* + F_2 (x^*)^{\otimes 2} = 0$, so the condition in Assumption I.2 is also satisfied if $\mu_P(F_{1,s}) \neq 0$. This implies that, given a system that has a locally exponentially stable equilibrium x^* , as long as s is chosen in a sufficiently small neighborhood of x^* , the stability conditions above are satisfied and the Carleman linearization can be applied to yield an efficient quantum algorithm. This makes the pivot-shifted Carleman linearization a powerful tool for simulating stable nonlinear systems around their stable equilibria, even when the original system does not satisfy the standard Carleman criteria.*

The formal version of the above theorem is stated as Theorem IV.1 in Section IV. The proof consists of two main parts. First, we transform the original system into a shifted and rescaled system that satisfies the desired stability condition. Second, we apply Carleman linearization to the transformed system and analyze the resulting quantum algorithm. The first part involves constructing block encodings of the coefficient matrices of the shifted system and efficiently transforming the initial and final states between the original and shifted variables. These ingredients are discussed mainly in Section II. The second part establishes convergence of the Carleman approximation for the shifted system and derives the corresponding quantum query complexity. In this part, we relax the assumptions on initial value used in [27]. In particular, instead of requiring $R_P = \frac{1}{-\mu_P(F_1)} \left(\|F_2\|_P \|x(0)\|_P + \frac{\|F_0\|_P}{\|x(0)\|_P} \right) < 1$, our analysis can be applied to any $\|v(0)\|_P < 1$. This removes the dependence on a lower bound for $\|x(0)\|_P$. In addition, while [27] focuses on history state preparation, our analysis targets final state preparation and achieves a query complexity $\tilde{\mathcal{O}}(\sqrt{T})$, improving over the best final state complexity $\tilde{\mathcal{O}}(T)$ for Carleman linearization in [28].

Although Theorem IV.1 provides long time convergence guarantees for systems that become stable after pivot shifting, the choice of pivot is crucial and may require prior knowledge of the dynamics. For systems that are inherently unstable, or for which no practical pivot choice stabilizes the shifted dynamics, pivot-shifted Carleman linearization can still be useful for improving short time convergence behavior. In this regime, we choose the pivot to be the initial condition, $s = x(0)$, so that the shifted variable satisfies $u(0) = 0$. This leads to the following short time convergence and query complexity guarantee.

Theorem I.5 (Informal complexity for general shifted systems). *Choose $s = x(0)$ and $Q = I$. Then there exists $t^* > 0$, depending on the coefficients F_i and the initial condition $x(0)$, such that for any $T \leq t^*$, there is a quantum algorithm that outputs an ϵ -approximation of the final state $|x(T)\rangle$ using*

$$\tilde{\mathcal{O}} \left(\frac{(1 + \|x(0)\|)^2 \sqrt{\|x(T) - x(0)\|^2 + \|x(0)\|^2} \max_{t \in [0, T]} \|x(t) - x(0)\| T^2}{\|x(T)\| \|x(T) - x(0)\|^2 \epsilon} \right)$$

queries the block encodings of F_i and the state-preparation oracle for $|x(0)\rangle$. Here, $\tilde{\mathcal{O}}(\cdot)$ suppresses logarithmic factors and constants associated with the block encoding normalizations and condition parameters of the transformed system.

The formal version of the above theorem is stated as Theorem IV.2 in Section IV. We note that the above theorem does not impose any stability structure on the shifted system, and therefore applies to a much broader class of dynamics than standard Carleman linearization. In traditional Carleman linearization, convergence may fail even on short time intervals when the stable condition is not satisfied. In contrast, by choosing $s = x(0)$, the shifted variable $u = x - s$ starts from zero. This can substantially improve the short time convergence behavior of the Carleman approximation, even when the underlying dynamics are unstable. The admissible short-time interval, however, may shrink when the shifted coefficients have a large overall scale. The analysis of the above theorem builds on the quantum linear differential equation solver in [28]. By slightly refining the upper bound on the matrix exponential of the Carleman linearized matrices, improved upon the estimation in [28, Lemma 16], we obtain a quadratic dependence on the evolution time T for general dynamics. We note that, when $x(T)$ is very close to $x(0)$, the factor $1/\|x(T) - x(0)\|^2$ in the complexity can become large. This scaling arises from the cost of the quantum linear solver applied to the Carleman-linearized system: when the target solution has norm close to zero, the success probability of preparing the normalized solution state can be small, and additional queries are needed to amplify this probability.

B. Related works

Several approaches have been developed for quantum algorithms for nonlinear differential equations. Early work by Leyton and Osborne [25] incorporates quadratic nonlinearities through the amplitude of two copies of the solution

state. The subsequence time-marching procedure requires multiple fresh copies of the solution state at each time step. Due to the no-cloning theorem, the resources required by this algorithm scale exponentially with time T and the inverse precision $1/\epsilon$, although only polylogarithmically with the dimension n under suitable sparsity assumptions. Numerous subsequent developments have sought to improve the dependence on time and precision, primarily for stable systems. For example, Carleman linearization has emerged as one of the most prominent frameworks: it systematically embeds nonlinear dynamics into a higher-dimensional linear system and admits rigorous error analysis. The quantum Carleman linearization approach was initially proposed by Liu et al. [26], who showed that dissipative quadratic nonlinear differential equations satisfying a negative log-norm condition together with the Reynolds-type condition in Eq. (2) can be solved efficiently using Carleman linearization, the quantum linear systems algorithm (QLSA), and a first-order forward Euler method, with complexity for final state preparation scales as $\tilde{\mathcal{O}}(T^2/\epsilon)$. This was later improved by Krovi [28] to $\tilde{\mathcal{O}}(T \text{ poly log}(1/\epsilon))$ by using a higher-order truncated Taylor-series solver for the resulting linear system. More recently, Wu et al. [29] extended the applicable regime to certain nonresonant systems through a refined spectral analysis of the Carleman matrix, while Jennings et al. [27] replaced the negative log-norm assumption with the more general stability condition in Eq. (4) by introducing a Lyapunov transform prior to the Carleman lifting. Unlike previous algorithms that output an approximation of the final state $|x(T)\rangle$, Jennings et al. [27] achieve an $\mathcal{O}(\text{poly log}(T/\epsilon))$ scaling for preparing an approximation to the history state proportional to $[x(0); x(h); \dots; x(Mh)]$. The history state preparation is naturally based on the "all at once" formulation, whereas extracting the final state requires additional padding and amplitude amplification procedure to boost the success probability of measuring the final state. In addition, all of these work focus on dissipative, stable or marginally stable dynamics, and do not provide theoretical guarantees for unstable ODE systems where $\alpha(F_1) > 0$. In contrast, our paper develops a modified Carleman method for unstable system. Related developments have also shown how boundary conditions can be incorporated into quantum differential equation algorithms through explicit block encodings [32] or penalty projection methods [33]. In addition, Carleman-type constructions have been extended from quadratic ordinary differential equations to polynomial nonlinear systems of arbitrary order [34]. Beyond Carleman linearization, other frameworks have also been explored for nonlinear dynamics on quantum computers. These include the Koopman–Neumann approach [22], which reformulates the dynamics as a linear evolution on observables and allows flexible choices of basis functions such as Fourier expansions [35]; the homotopy perturbation method [36], which reduces the problem to solving a sequence of linearized equations; and quantum algorithms for nonlinear Schrödinger-type equations [37].

Our work is related to recent efforts that introduce shifting or piecewise embedding ideas into Carleman linearization. Endo and Takahashi [38] proposed a *pivot-switching* method, in which the pivot state s is repeatedly updated as the trajectory evolves, while the Carleman lifting is still performed about the origin. We emphasize that, despite the similar nomenclature, their method differs from ours in two essential respects: they switch pivots dynamically over the simulation, whereas the present work uses a single static shift; and their generator expansion is performed only locally, whereas we Carleman-lift directly around the shifted pivot. Although the strategy of [38] can extend the accessible simulation time, it generally produces a linear approximation with a non-sparse coefficient matrix, which results in a substantial increase in the cost of block encoding and quantum simulation. In addition, during the pivot-switching step, the Carleman linearization requires block encodings of both the new coefficient matrix and the updated initial state. To the best of our knowledge, it remains unclear whether these objects can be prepared efficiently. Closely related ideas were explored in the global piecewise Carleman embedding framework of [39], which showed that some chaotic systems can be approximated by Carleman linearization if pivot shifts are performed sufficiently frequently. Shifted formulations also appear in quantum algorithms based on lattice Boltzmann methods [40]. In the quantum setting, however, repeated pivot updates can introduce substantial overhead, since they require measurements to estimate both the current state and the next pivot, while the resulting loss of sparsity may significantly increase the cost of block encoding. In our work, we mainly focus on a single pivot shift, which avoids the overhead of repeated measurements and pivot updates. To the best of our knowledge, it remains unclear how to implement pivot switching efficiently in practice. Although we do not consider switching between pivot points, our results establish a theoretical foundation for the convergence of a single step in [38, 39]. For unstable systems, our analysis further provides a theoretical characterization of an upper bound on the switching time. We will discuss the potential of multiple pivot shifts (pivot switching) in Section VI.

The key primitive underlying Carleman-based algorithm is an efficient quantum solver for linear differential equations. Existing quantum algorithms for linear differential equations are typically based on the QLSA [16], time-marching methods [12], or reformulations in terms of Hamiltonian simulation [13, 14, 41]. The optimal query complexity for general linear differential equations is limited by the $\Omega(T)$ lower bound for Hamiltonian simulation [42]. In contrast, recent works have shown that for certain classes of linear differential equations, we can obtain fast forwarded complexity [43]. In particular, for stable linear systems, the complexity of history state preparation can be reduced to $\mathcal{O}(\sqrt{T})$ [44]. For dissipative linear systems, the query complexity of final state preparation can be improved to $\tilde{\mathcal{O}}(\sqrt{T})$ via QLSA [45], and the dependence on T can be eliminated using LCHS-based or time-marching approaches [46]. In

	Method	Stability	Query complexity		Remark
			History state	Final state	
Linear ODEs	Truncated Taylor [15, 28]	$\max_t \ e^{At}\ = \mathcal{O}(1)$	$\tilde{\mathcal{O}}(T \text{ poly log}(1/\epsilon))$	$\tilde{\mathcal{O}}(T \text{ poly log}(1/\epsilon))$	QLSA based
	LCHS/Schrödingerization [13, 41]	$A(t) + A(t)^\dagger < 0$	$\tilde{\mathcal{O}}(T \text{ poly log}(1/\epsilon))$	$\tilde{\mathcal{O}}(T \text{ poly log}(1/\epsilon))$	Hamiltonian simulation
Fast-forwarded Linear ODEs	Fast-forwarded Taylor [44]	$\alpha < 0$	$\tilde{\mathcal{O}}(T^{1/2}(\log(1/\epsilon))^2)$	$\tilde{\mathcal{O}}(T^{3/4}(\log(1/\epsilon))^2)$	QLSA based
	Fast-forwarded Euler/Dyson [45]	$A(t) + A(t)^\dagger < 0$	$\mathcal{O}(\log(T)(\log(1/\epsilon))^2)$	$\tilde{\mathcal{O}}(T^{1/2}(\log(1/\epsilon))^2)$	QLSA based
	Fast-forwarded LCHS [46]	$A(t) + A(t)^\dagger < -2\eta < 0$ $T = \tilde{\Omega}(\frac{1}{\eta})$	$\mathcal{O}(\log^3(1/\epsilon))$	$\mathcal{O}(\log^3(1/\epsilon))$	Hamiltonian simulation
Carleman-based Nonlinear ODEs	Liu et. al. [26]	$\mu < 0, R < 1$	/	$\tilde{\mathcal{O}}(T^2/\epsilon)$	Forward Euler
	Krovi [28]	$\mu < 0, R < 1$	/	$\tilde{\mathcal{O}}(T \text{ poly log}(1/\epsilon))$	Truncated Taylor
	Jennings et al. [27]	$\alpha < 0, R_P < 1$	$\mathcal{O}(\text{poly log}(T/\epsilon))$	/	Fast-forwarded Taylor [44, 45]
	This work	Assumptions I.1 and I.2	/	$\tilde{\mathcal{O}}(\sqrt{T} \text{ poly log}(1/\epsilon))$	Fast-forwarded Taylor [45]

Table I: Comparison of quantum algorithms for linear and nonlinear differential equations. Here, α denotes the spectral abscissa and μ denotes the logarithmic norm of the linear part of the differential equation. The table focuses on the dissipative or stable setting and the time-independent case.

this work, we analyze the QLSA-based Carleman linearization with the linear differential equation solver developed in [45]. Our analysis is tailored to final state preparation and achieves a query complexity $\tilde{\mathcal{O}}(\sqrt{T})$ using [45]. This improves over the final state preparation cost obtained from the linear differential equation solvers used in [27], namely $\tilde{\mathcal{O}}(T^{3/4})$ scaling based query complexity on [44]. Moreover, we formulate the query complexity in terms of the condition number $\kappa(Q)$, rather than the norm of Q , making the bound invariant under rescaling of Q . Such rescaling invariance is essential for a consistent treatment of block encoding normalization factors.

C. Organization

The remainder of the paper is organized as follows. In Section II, we introduced the notation, norm properties and quantum primitives. In Section III, we present the pivot-shifted Carleman linearization algorithm. In Section IV, we analyze the error convergence and complexity. In Section V, we demonstrate the performance of our algorithm through numerical experiments. We summarize our results and discuss future directions in Section VI.

II. PRELIMINARIES

a. Norm and Properties Throughout this paper, we use $\|\cdot\|$ to denote the Euclidean vector norm or the induced matrix norm. In this section, we introduce the property of the weighted norm for matrices in $\mathbb{R}^{n \times 1}$, $\mathbb{R}^{n \times n}$ and $\mathbb{R}^{n \times n^2}$. Given a vector $\psi \in \mathbb{R}^n$, we denote $|\psi\rangle = \psi/\|\psi\|$ as the normalized quantum state.

Given a positive definite matrix $O \succeq 0$, we define the O -induced inner product by

$$\langle x, y \rangle_O = x^\dagger O y. \quad (7)$$

Then,

- For $x \in \mathbb{R}^{n \times 1}$, the weighted norm is

$$\|x\|_O = \sqrt{\langle x, x \rangle_O}. \quad (8)$$

- For $F \in \mathbb{R}^{n \times n}$, the weighted matrix norm

$$\|F\|_O := \max_{x \neq 0} \frac{\|Fx\|_O}{\|x\|_O} = \max_{x \neq 0} \frac{\|\sqrt{O}Fx\|}{\|\sqrt{O}x\|} = \max_{y \neq 0} \frac{\|\sqrt{O}F\sqrt{O}^{-1}y\|}{\|y\|} = \|\sqrt{O}F\sqrt{O}^{-1}\|. \quad (9)$$

- For $G \in \mathbb{R}^{n \times n^2}$, the norm follows

$$\|G\|_O := \max_{x \neq 0} \frac{\|Gx\|_O}{\|x\|_O} = \|O^{1/2}G(O^{-1/2} \otimes O^{-1/2})\|. \quad (10)$$

The logarithmic norm can also be defined from the vector norm. For a matrix $F \in \mathbb{R}^{n \times n}$, its log norm is defined as

$$\mu(F) = \frac{1}{2} \max_i \lambda_i(F + F^\dagger). \quad (11)$$

Correspondingly, the weighted log norm follows

$$\mu_O(F) = \max_{x \neq 0} \operatorname{Re} \left(\frac{\langle Fx, x \rangle_O}{\langle x, x \rangle_O} \right) = \lim_{h \rightarrow 0^+} \frac{\|I + hF\|_O - 1}{h} = \lim_{h \rightarrow 0^+} \frac{\|I + h\sqrt{O}F\sqrt{O}^{-1}\| - 1}{h} = \mu(\sqrt{O}F\sqrt{O}^{-1}). \quad (12)$$

For two functions f, g that characterize complexity scaling, we use the notation $f = \mathcal{O}(g)$ if there exists some constant $c > 0$ such that $f \leq cg$. We write $f = \Theta(g)$ or $f \sim g$ if both $f = \mathcal{O}(g)$ and $g = \mathcal{O}(f)$ hold. Additionally, $f = \tilde{\mathcal{O}}(g)$ denotes the polylogarithmic factors are suppressed, i.e., $f = \mathcal{O}(g \text{ poly log}(g))$.

b. Quantum primitive Quantum hardware naturally implements unitary evolution. However, most matrices in scientific computing do not satisfy the unitary property. A natural idea is therefore to construct a larger unitary matrix so that the non unitary matrix A becomes the upper left block, i.e.

$$U_A \approx \begin{pmatrix} A/\alpha & * \\ * & * \end{pmatrix}. \quad (13)$$

This is the key idea behind the block encoding, an important building block in quantum algorithm design.

Definition II.1 (Block Encoding). *Given an n -qubit operator A , if there exists $\alpha, \epsilon > 0$ and a n -qubit unitary U_A such that*

$$\|A - \alpha(\langle 0|^{\otimes a} \otimes I_n)U_A(|0^a\rangle \otimes I_n)\| \leq \epsilon \quad (14)$$

then U_A is called an (α, a, ϵ) -block encoding of A . The block encoding is exact when $\epsilon = 0$.

While block encoding is not guaranteed to be efficient for arbitrary dense matrices, linear combinations of unitaries (LCU) provides flexibility in constructing suitable block encodings [3, Lemma 52]. We introduce the slightly generalized version with different normalizing factors stated in [47, Lemma 5].

Lemma II.2 (Linear combination of unitaries). *Suppose $A := \sum_{j=1}^m y_j A_j \in \mathbb{C}^{2^n \times 2^n}$, where $A_j \in \mathbb{C}^{2^n \times 2^n}$ and $y_j > 0$ for all $j \in \{1, \dots, m\}$. Let U_j be an (α_j, a, ϵ) -block-encoding of A_j and $s = \sum_{j=1}^m y_j \alpha_j$. Define the state preparation oracle pair as*

$$\mathbf{Prep} : |0\rangle \rightarrow \sum_{j=0}^{m-1} \sqrt{\frac{\alpha_j y_j}{s}} |j\rangle, \quad (15)$$

and the select oracle as

$$\mathbf{Select} = \sum_{j=0}^{m-1} |j\rangle\langle j| \otimes U_j. \quad (16)$$

Then the matrix

$$(\mathbf{Prep}^\dagger \otimes I)\mathbf{Select}(\mathbf{Prep} \otimes I) \quad (17)$$

is an $(\sum_{j=1}^m \alpha_j y_j, a + \log(m), \sum_{j=0}^{m-1} \alpha_j y_j \epsilon)$ -block encoding of A .

Additionally, the matrix inverse can be implemented through the QLSA with the following query complexity.

Lemma II.3. ([11, Theorem 11]) *Suppose a matrix $A \in \mathbb{C}^{2^n \times 2^n}$ with $\|A\| = 1$ and $\|A^{-1}\| = \kappa$. Given a block encoding oracle of the matrix A and a state preparation oracle for $|b\rangle$, then the approximation of the normalized state $|A^{-1}b\rangle$ with precision ϵ can be produced with*

$$\mathcal{O}(\kappa \log(1/\epsilon)) \quad (18)$$

calls to the oracles.

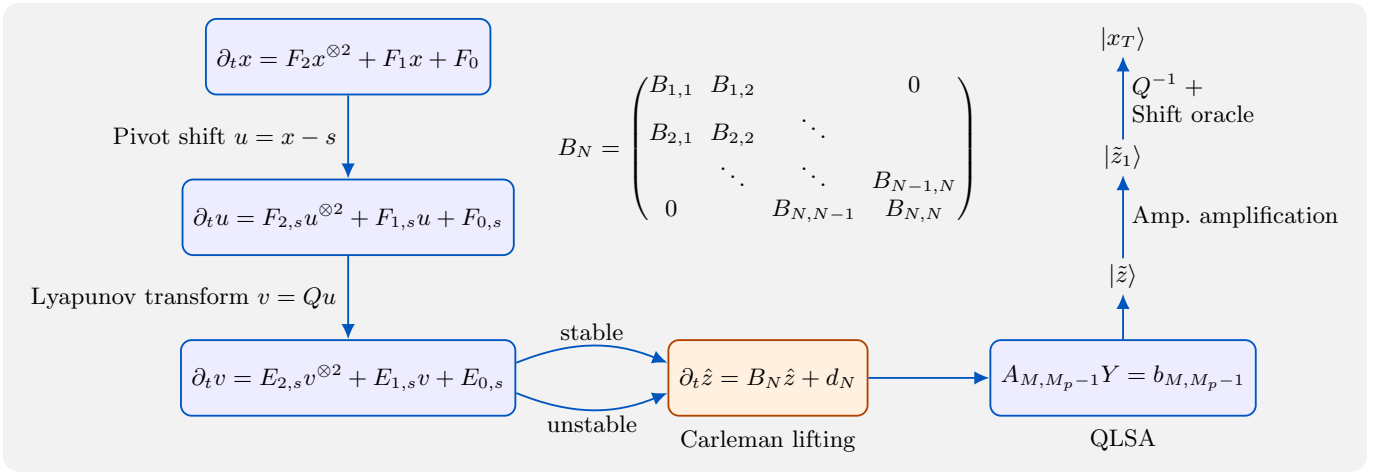


Figure 1: Flowchart for the pivot-shifted Carleman linearization algorithm.

c. *Prepare the shifted initial state* To ensure efficient encoding of the problem in Eq. (1) onto quantum computer, we make the following assumptions on the input model:

- We assume F_2, F_1, F_0 are block encoded with normalizing factors $\alpha_{F_2}, \alpha_{F_1}, \alpha_{F_0}$.
- We assume the matrix Q that is proportional to \sqrt{P} are block encoded with normalizing factor $\alpha_Q = \mathcal{O}(\|Q\|)$. We denote the condition number of Q by $\kappa_Q = \|Q\|\|Q^{-1}\|$.
- We assume $\|x_0\|$ is known and the normalized vector $|x_0\rangle$ can be efficiently prepared by an initial state preparation oracle, meaning $|x_0\rangle = O_{x_0}|0\rangle$ for some unitary O_{x_0} that can be implemented efficiently.
- Given the pivot s , we assume $\|s\|$ is known and a normalized state $|s\rangle = s/\|s\|$ can be efficiently prepared by an initial state preparation oracle O_s .

Given a pivot state s and the shifted variable $u = x - s$, Eq. (1) can be rewritten as Eq. (3) with

$$F_{2,s} = F_2, \quad F_{1,s} = F_1 + F_2(s \otimes I_n + I_n \otimes s), \quad F_{0,s} = F_2 s^{\otimes 2} + F_1 s + F_0. \quad (19)$$

The cost of constructing $F_{2,s}$, $F_{1,s}$, and $F_{0,s}$ and the state preparation oracle for the shifted initial state $|u(0)\rangle$ are summarized in the following lemma.

Lemma II.4. *Assume access to the the block encoding oracle $O_{F_2}, O_{F_1}, O_{F_0}$, the state preparation oracles O_x, O_s , as introduced above. The following hold:*

- The block encoding oracle for $F_{0,s}, F_{1,s}, F_{2,s}$ can be constructed with normalizing factor $\alpha_{F_{2,s}} = \alpha_{F_2}$, $\alpha_{F_{1,s}} = \alpha_{F_1} + 2\|s\|\alpha_{F_2}$ and $\alpha_{F_{0,s}} = \alpha_{F_0} + \alpha_{F_1}\|s\| + \alpha_{F_2}\|s\|^2$.
- The shifted initial state $|u(0)\rangle = |x(0) - s\rangle$ can be prepared with $\mathcal{O}\left(\frac{\sqrt{\|x(0)\|^2 + \|s\|^2}}{\|x(0) - s\|}\right)$ queries to O_{x_0} and O_s .
- The final state $|x(T)\rangle$ can be shifted back from $|u(T)\rangle$ with $\mathcal{O}\left(\frac{\sqrt{\|x(T) - s\|^2 + \|s\|^2}}{\sqrt{p}\|x(T)\|}\right)$ queries to the preparation oracles $O_{u(T)}$ and O_s , where $O_{u(T)}$ is the state preparation oracle such that

$$O_{u(T)}|0^{m+k}\rangle = \sqrt{p}|0^k\rangle|u(T)\rangle + \sqrt{1-p}|\perp\rangle, \quad \langle 0^k|\perp\rangle = 0.$$

The detailed construction and cost of each oracle can be found in Section A. In the above theorem, $O_{u(T)}$ will be constructed from the Carleman linearization of the shifted system. The detailed discussion and estimation of p can be found in Section A.

III. DETAILS OF THE PIVOT-SHIFTED ALGORITHM

We present the pivot-shifted Carleman linearization, incorporating the Lyapunov transform in [27], for the quadratic nonlinear differential equation in Eq. (1). Our approach applies the Carleman linearization directly around the pivot s after expanding the generator at the same point. This formulation leads to a sparser lifting matrix, is compatible with single-shot measurement and allows us to combine it with the quantum algorithms designed for stable nonlinear differential equations. The algorithm consists of four steps as illustrated in Fig. 1:

- (1) **Pivot shift.** Given a suitable pivot vector $s \in \mathbb{R}^n$, we apply a pivot-shift transformation $u = x - s$, with initial condition $u(0) = x(0) - s$. Under this change of variables, Eq. (1) can be rewritten as

$$\partial_t u = F_{2,s} u^{\otimes 2} + F_{1,s} u + F_{0,s}, \quad (20)$$

where the shifted coefficient matrices are given by Eq. (19). The block encoding oracles for $F_{2,s}$, $F_{1,s}$, and $F_{0,s}$, as well as the state preparation oracle for the shifted initial state $u(0)$, can be constructed efficiently, as summarized in Lemma II.4. When the prior information about a stable region is available, the pivot s can be chosen in that region to improve the stability of the shifted dynamics. In the absence of such information, or when the system is unstable, a natural choice is $s = x(0)$, as in [39]. This choice does not generally stabilize the system, but it gives $u(0) = 0$ and supports short time convergence of the Carleman approximation.

- (2) **Lyapunov Transform.** With a *positive definite matrix* Q , we then consider the change of variable

$$v = Qu. \quad (21)$$

Under this transformation, the differential equation becomes

$$\partial_t v = E_{2,s} v^{\otimes 2} + E_{1,s} v + E_{0,s}, \quad (22)$$

where the coefficient matrices are given by

$$E_{2,s} = QF_{2,s}(Q^{-1} \otimes Q^{-1}), E_{1,s} = QF_{1,s}Q^{-1}, E_{0,s} = QF_{0,s}, v_0 = Qu_0. \quad (23)$$

This transform is introduced to enhance the stability properties of the linearized system. Under Assumptions I.1 and I.2, we choose $Q = \sqrt{P}/\gamma$, following [27], so that the linearized differential equation is dissipative and that can be solved efficiently by a quantum linear differential equation solver. For general systems where the prior knowledge of the underlying system might not be available, we also provide analysis when $Q = I$.

- (3) **Carleman lifting.** We truncate the Carleman Linearization at order N and denote the resulting lifted solution as $\hat{z} = (\hat{z}_k)_{k=1}^N$ such that

$$\frac{d}{dt} \hat{z} = \frac{d}{dt} \begin{bmatrix} \hat{z}_1 \\ \hat{z}_2 \\ \vdots \\ \hat{z}_N \end{bmatrix} = \begin{bmatrix} B_{1,1} & B_{1,2} & 0 & \cdots & 0 \\ B_{2,1} & B_{2,2} & B_{2,3} & \ddots & \vdots \\ 0 & B_{3,2} & B_{3,3} & \ddots & 0 \\ \vdots & \ddots & \ddots & \ddots & B_{N-1,N} \\ 0 & \cdots & 0 & B_{N,N-1} & B_{N,N} \end{bmatrix} \begin{bmatrix} \hat{z}_1 \\ \hat{z}_2 \\ \vdots \\ \hat{z}_N \end{bmatrix} + \begin{bmatrix} E_{0,s} \\ 0 \\ \vdots \\ 0 \end{bmatrix} =: B_N \hat{z} + d_N. \quad (24)$$

The initial condition approximates the lifted exact solution

$$\hat{z}(0) \approx [v_0; v_0^{\otimes 2}; \cdots; v_0^{\otimes N}].$$

This block tridiagonal structure is inherited from the quadratic form of the differential equation. For admissible indices j from 1 to N , the blocks are given by

$$\begin{aligned} B_{j,j+1} &= E_{2,s} \otimes I^{\otimes(j-1)} + I \otimes E_{2,s} \otimes I^{\otimes(j-2)} + \cdots + I^{\otimes(j-1)} \otimes E_{2,s}, \\ B_{j,j} &= E_{1,s} \otimes I^{\otimes(j-1)} + I \otimes E_{1,s} \otimes I^{\otimes(j-2)} + \cdots + I^{\otimes(j-1)} \otimes E_{1,s}, \\ B_{j,j-1} &= E_{0,s} \otimes I^{\otimes(j-1)} + I \otimes E_{0,s} \otimes I^{\otimes(j-2)} + \cdots + I^{\otimes(j-1)} \otimes E_{0,s}. \end{aligned} \quad (25)$$

The truncation order N is chosen so that the Carleman truncation error is below the accuracy ϵ . This choice also contributes to the query complexity of the quantum solvers for the linearized differential equation. The detailed discussion on error analysis can be found in Section IV A.

encoding oracles for F_2 , F_1 , F_0 and Q , together with state preparation oracles for the initial state $|x(0)\rangle$ and the pivot $|s\rangle$. The complexity of the algorithm is measured in terms of the number of queries to these oracles.

We establish sublinear time dependence for systems that become stable after pivot shift. For general systems that probably remain unstable even after pivot shift, we proved the short time convergence. We begin with the stable case where we choose the Lyapunov transform properly so that $\mu(B_N) < 0$, defined in Eq. (11).

Theorem IV.1 (Main result 1: stable system). *Under Assumptions I.1 and I.2, we choose $Q = \sqrt{P}/\gamma$ with rescaling parameter $\gamma \in (\zeta_-^P, r_+^P)$, where*

$$r_{\pm}^P = \frac{-\mu_P(F_{1,s}) \pm \sqrt{\mu_P(F_{1,s})^2 - 4\|F_{2,s}\|_P\|F_{0,s}\|_P}}{2\|F_{2,s}\|_P}, \quad \zeta_{\pm}^P = \frac{-4\mu_P(F_{1,s}) - \sqrt{16\mu_P(F_{1,s})^2 - 60\|F_{0,s}\|_P\|F_{2,s}\|_P}}{6\|F_{2,s}\|_P}. \quad (32)$$

Here, $F_{i,s}$ are defined in Eq. (19) with $\mu_P(\cdot)$ and $\|\cdot\|_P$ defined in Section II.

Denote the Carleman truncation order N . Suppose the initial value $\|v(0)\| < 1$, then for arbitrary $\epsilon > 0$, there exists an efficient quantum algorithm the output an ϵ -approximation of the normalized quantum state $|x(T)\rangle$ using

- $\tilde{O}\left(\frac{\sqrt{\|x(T)-s\|^2+\|s\|^2}}{\|x(T)\|} \frac{\kappa_Q\sqrt{T}g_v}{\sqrt{|C_E|}} \alpha_E \text{poly log}(4\kappa_Q/\epsilon)\right)$ queries to O_{F_i} ,
- $\tilde{O}\left(\frac{\sqrt{\|x(T)-s\|^2+\|s\|^2}}{\|x(T)\|} \frac{\sqrt{\|x(0)\|^2+\|s\|^2}}{\|x(0)-s\|} \frac{\kappa_Q^2\sqrt{T}g_v}{\sqrt{|C_E|}} \alpha_E \text{poly log}(4\kappa_Q/\epsilon)\right)$ queries to the state preparation oracle of O_{x_0} and O_s ,
- $\tilde{O}\left(\frac{\sqrt{\|x(T)-s\|^2+\|s\|^2}}{\|x(T)\|} \frac{\kappa_Q^3\sqrt{T}g_v}{\sqrt{|C_E|}} \alpha_E \text{poly log}(4\kappa_Q/\epsilon)\right)$ queries to the block encoding of Q ,

where α_E, g_v are defined in Section IA. Here, the constants are defined with weighted norm and logarithmic norm on $O = P/\gamma^2$,

$$C_E := \max\{4\mu_O(F_{1,s}) + 3\|F_{2,s}\|_O + 5\|F_{0,s}\|_O, \mu_O(F_{1,s}) + \|F_{2,s}\|_O + \|F_{0,s}\|_O\} < 0 \quad (33)$$

$$\alpha_E = \alpha_{F_0}\alpha_Q + \alpha_{F_1}(\|s\|\alpha_Q + \kappa_Q) + \alpha_{F_2}\left(\|s\|^2\alpha_Q + 2\|s\|\kappa_Q + \frac{\kappa_Q^2}{\alpha_Q}\right). \quad (34)$$

The condition in Theorem IV.1 requires prior knowledge of both the stable region and a suitable transformation matrix Q . Under these assumptions, the shifted system provably satisfies the conditions needed both for the convergence of the Carleman linearization and for the efficient application of a QLSA-based solver for the resulting dissipative linear differential equation.

The next case is when the underlying system is unstable or no prior knowledge about the stable region is available. In this case, we use the classical ‘‘shift-to-origin’’ trick to stabilize the Carleman linearization [48, 49] by choosing the pivot to be the initial state, $s = x(0)$, which guarantees good local behavior and thus supports convergence of the Carleman approximation over short time scales. However, since the shifted system is not guaranteed to be stable, we can only expect short-term convergence of the Carleman linearization, and the complexity of the resulting QLSA-based linear differential equation solver will have a worse dependence on the final time T . The complexity in this case is summarized in the following theorem.

Theorem IV.2 (Main result 2: unstable system). *Choose $s = x(0)$ and $Q = I$. Then, there exists $t^* > 0$ such that: 1. $\|v(t)\| < 1$ for all $0 \leq t \leq t^*$; 2. For any $T < t^*$, there exists an efficient quantum algorithm to solve the quadratic ODE and output a quantum state ϵ -close to the final state $|x(T)\rangle$ with*

$$\tilde{O}\left(\frac{\sqrt{\|x(T) - x(0)\|^2 + \|x(0)\|^2}}{\|x(T)\|} \frac{(\alpha_{F_0} + \alpha_{F_1} + \alpha_{F_2})(1 + \|x(0)\|)^2 \|F_2\| T^2 g_v \text{polylog}(n)}{\|x(T) - x(0)\|\epsilon}\right)$$

queries to O_{F_i} and $O_{x(0)}$.

The performance guarantee holds up to a time point t^* , which may decrease when the shifted coefficient scale, namely, when $\sum_i \|F_{i,s}\|$ becomes large.

We put the proof in the following part of this section. The complexity analysis consists of four main steps:

- *Step 1: Preparation of oracles for the shifted system.*

This corresponds to the first two steps of the algorithm, namely the pivot shift and the Lyapunov transform. Specifically, we need to construct the block encoding oracles for $F_{2,s}$, $F_{1,s}$, and $F_{0,s}$, as well as the state preparation oracle for $|u(0)\rangle$. These are constructed using the block encoding for F_2 , F_1 , and F_0 , along with the state preparation oracle for $|s\rangle$ and $|x(0)\rangle$. The complexity of this step is analyzed in Section II Lemma II.4.

- *Step 2: Convergence of the Carleman Linearization.*

This corresponds to the third step of the algorithm, where we analyze the error convergence of the Carleman linearization for the shifted system. We derive explicit bounds on the truncation order N required to achieve a target accuracy ϵ for approximating the solution at time T . The analysis is presented in Section IV A. For stable systems, this result can be stated in a consistent form with prior knowledge, which is given in Proposition IV.3. For unstable systems, we only expect short time convergence, and the convergence result is stated in Proposition IV.4.

- *Step 3: Complexity of solving the lifted linear differential equations.*

This corresponds to the fourth step of the algorithm, where we analyze the complexity of applying the QLSA-based linear differential equation solver to the lifted system obtained from the Carleman linearization. In this step, we will mainly rely on the algorithms in [28, 45] to obtain a better dependence on the final time T . The complexity result is summarized in Section IV B Proposition IV.7 for stable systems and in Proposition IV.8 for unstable systems.

- *Step 4: Putting everything together and shifting the state back.*

Finally, we combine the results from the previous steps to derive the overall complexity of the pivot-shifted Carleman linearization algorithm for both stable and unstable systems as stated in Theorem IV.1, and Theorem IV.2. Here, we also need to analyze the complexity of shifting the state back from $|v(T)\rangle$ to $|x(T)\rangle$ and estimating $\|x(T)\|$. This is done in Section IV C.

A. Convergence of the Carleman linearization

In this section, we analyze the convergence of the Carleman linearization for the shifted system in both the stable and unstable cases. This completes the second step of the complexity analysis outlined above. We start with the error caused by the Carleman linearization with truncation order N . We denote the exact lifted solution from the Carleman linearization with Lyapunov transform in (24) algorithms as $z(t) = (z_k(t))_{k \geq 1}$ where $z_k(t) = v(t)^{\otimes k}$. Following the algorithm stated in Section III, we denote the corresponding error vectors as $\xi = \xi(t) := z(t) - \hat{z}(t)$, satisfying the equation

$$\partial_t \xi = B_N \xi + \hat{d}_N, \quad (35)$$

with the matrix B_N in Eq. (24), and

$$\hat{d}_N = [0; 0; \dots; 0; B_{N,N+1} z_{N+1}(t)]. \quad (36)$$

By analyzing the bound on $\|\xi_1(t)\| := \|z_1(t) - \hat{z}_1(t)\|$, we can obtain the error bound for approximating $v(t)$.

First, for the stable solution, as will be shown in Lemma IV.5, under Assumptions of Theorem IV.1, the solution $v(t)$ of the shifted system can be bounded by a constant that is strictly less than 1 for all $t \in [0, T]$. This bound on the solution allows us to obtain the exponential decay of the Carleman error with respect to the truncation order N , which in turn leads to a logarithmic scaling of N with T/ϵ to achieve an ϵ -accurate solution. The precise statement is given in the following proposition.

Proposition IV.3 (Stable system). *Under Assumptions I.1 and I.2, we choose $Q = \sqrt{P}/\gamma$ with rescaling parameter $\gamma \in (\zeta_-^P, r_+^P)$ and denote the Carleman truncation order N . Suppose the initial value $\|v(0)\| < 1$. Then,*

$$\max_{t \in [0, T]} \|v(t)\| \leq \max \left\{ \|v(0)\|, \frac{r_-^P}{\gamma} \right\} < 1.$$

Furthermore, the Carleman embedding error vector can be bounded:

$$\|\xi(t)\| \leq tN\gamma \|F_{2,s}\|_P \max_{t \in [0, T]} \|v(t)\|^{N+1}, \quad (37)$$

for $j = 1, \dots, k$. The relative error can be bounded by ϵ , meaning $\|\xi_1(T)\| \leq \|\xi(T)\| \leq \epsilon\|v(T)\|$, by choosing the truncation order

$$N = \Theta \left(\frac{\log(T\gamma\|F_{2,s}\|_P / (\|v(T)\|\epsilon))}{\log(1/\max_{t \in [0, T]} \|v(t)\|)} \right).$$

We provide the proof of Proposition IV.3 in Section IV A 1. Proposition IV.3 implies that, as long as $x(0) - s$ is sufficiently small and the system is stable, the truncation order N only needs to scale logarithmically with t/ϵ to achieve an ϵ -accurate solution.

Without Assumptions I.1 and I.2 and correct choice of Q , the system might not be a stable system, while we can still provide the bound for Carleman error vector for short time. When $\|v(0)\|$ is sufficiently small, combining the Carleman error with the solution bound, we can also obtain a logarithmic scaling of the truncation order N with t/ϵ to achieve an ϵ -accurate solution for the unstable system for short time, as shown in the following proposition.

Proposition IV.4 (Unstable system). *Choose $Q = I$ and pivot $s = x(0)$. Define*

$$t^* = \frac{1}{e(\|F_{1,s}\| + \|F_{0,s}\| + \|F_{2,s}\|)}.$$

Then, $\max_{t \in [0, t^*]} \|v(t)\| < 1$. In addition, the Carleman embedding error vector can be approximated as

$$\max_{t \in [0, t^*]} \|\xi(t)\| \leq tN^{3/2}\|F_{2,s}\| (t(\|F_{2,s}\| + \|F_{1,s}\| + \|F_{0,s}\|)e)^{N+1}. \quad (38)$$

Given $T \in [0, t^*]$, the relative error can be bounded by ϵ so that $\|\xi(T)\| \leq \epsilon\|v(T)\|$ by choosing the truncation order

$$N \geq \Theta \left(\frac{\log(T\|F_{2,s}\| / (\|v(T)\|\epsilon))}{\log(1/(t^*(\|F_{2,s}\| + \|F_{1,s}\| + \|F_{0,s}\|)e))} \right).$$

The proof of Proposition IV.3 is similar to that of Proposition IV.4. We put the proof of Proposition IV.4 in Appendix B.

1. Proof of Proposition IV.3

We first establish a bound on the solution $v(t)$ of the shifted system, which is crucial for analyzing the convergence of the Carleman linearization.

Lemma IV.5. *Under Assumptions I.1 and I.2. Consider $v(t)$ in Eq. (22). Define*

$$r_{\pm}^P = \frac{-\mu_P(F_{1,s}) \pm \sqrt{\mu_P(F_{1,s})^2 - 4\|F_{2,s}\|_P\|F_{0,s}\|_P}}{2\|F_{2,s}\|_P}. \quad (39)$$

Then,

$$\max_{t \in [0, T]} \|v(t)\| = \begin{cases} \|v(0)\| & \text{if } \|v(0)\| \in [\frac{1}{\gamma}r_{-}^P, \frac{1}{\gamma}r_{+}^P), \\ \frac{1}{\gamma}r_{-}^P & \text{if } \|v(0)\| \in [0, \frac{1}{\gamma}r_{-}^P). \end{cases} \quad (40)$$

In particular, if $\gamma \in (\zeta_{-}^P, r_{+}^P) \subset (r_{-}^P, r_{+}^P)$ and $\|v(0)\| < 1$, then $\max_{t \in [0, T]} \|v(t)\| \leq \max \left\{ \|v(0)\|, \frac{r_{-}^P}{\gamma} \right\} < 1$.

This bound in Lemma IV.5 is slightly more general than the results in [26, 27], as it does not require a positive lower bound on $\|u(0)\|$ (i.e., an assumption of the form $\delta < \|u(0)\|$ for some $\delta > 0$). For example, when $u(0) = 0 < r_{-}^P$, the solution is not controlled by its initial value, yet we can still obtain the uniform upper bound $\|u(t)\|_P < r_{-}^P$. The absence of a lower bound on $\|u(0)\|$ is consistent with the convergence radius statement in [39], while yielding a more precise mathematical formulation.

Under these conditions, the norm of the transformed solution remains uniformly bounded by 1 on $[0, T]$. This uniform bound enables us to establish the convergence of the Carleman linearization and prove Proposition IV.3 as follows.

Proof of Proposition IV.3. The Lyapunov transform matrix Q works as the preconditioner matrix to the Carleman linearization matrix B_N .

We recall the definition of the error vector $\xi(t)$ in Eq. (35) and Eq. (36):

$$\partial_t \xi = B_N \xi + \hat{d}_N,$$

with

$$\hat{d}_N = [0; 0; \cdots; 0; B_{N,N+1} v^{\otimes(N+1)}(t)].$$

where the block entries $B_{\cdot,\cdot}$ are defined in Eq. (25).

Notice that the error term $\|\xi(t)\|$ follows

$$\partial_t \|\xi\|^2 = \xi^\dagger (B_N + B_N^\dagger) \xi + \xi^\dagger \hat{d}_N + \hat{d}_N^\dagger \xi. \quad (41)$$

The first term can be estimated as

$$\begin{aligned} \xi^\dagger (B_N + B_N^\dagger) \xi &= \sum_j \xi_j^\dagger (B_{j,j} + B_{j,j}^\dagger) \xi_j + \sum_j \xi_{j+1}^\dagger (B_{j+1,j} + B_{j+1,j}^\dagger) \xi_j + \sum_j \xi_j^\dagger (B_{j+1,j}^\dagger + B_{j,j+1}) \xi_{j+1} \\ &\leq \sum_j 2\mu(B_{j,j}) \|\xi_j\|^2 + \sum_j 2\|B_{j+1,j}\| \|\xi_j\| \|\xi_{j+1}\| + \sum_j 2\|B_{j,j+1}\| \|\xi_j\| \|\xi_{j+1}\| \\ &\leq \sum_j 2j\mu(E_{1,s}) \|\xi_j\|^2 + 2j\|E_{0,s}\| \|\xi_j\| \|\xi_{j-1}\| + 2(j-1)\|E_{2,s}\| \|\xi_j\| \|\xi_{j-1}\| \\ &\leq \xi_G^\dagger (G + G^\dagger) \xi_G \leq 2\mu(G). \end{aligned} \quad (42)$$

In the second inequality, we use the definition of $B_{j,j}$, $B_{j,j+1}$, and $B_{j+1,j}$ in Eq. (25). In the last inequality, we define the vector $\xi_G = (\|\xi_i\|)_i$ and the tridiagonal matrix $G \in \mathbb{C}^{N \times N}$:

$$G_{j,j} = j\mu(E_{1,s}), G_{j-1,j} = j\|E_{0,s}\|, G_{j+1,j} = j\|E_{2,s}\|. \quad (43)$$

We denote the upper bound of the eigenvalues of $G + G^\dagger$ as C_E . By Gershgorin's circle theorem,

$$C_E \geq \begin{cases} 2G_{j,j} + (G_{j,j+1} + G_{j+1,j}) + (G_{j,j-1} + G_{j-1,j}) & \text{for } j = 2, \dots, N-1 \\ 2G_{1,1} + (G_{1,2} + G_{2,1}) & \text{for } j = 1 \\ 2G_{N,N} + (G_{N,N-1} + G_{N-1,N}) & \text{for } j = N \end{cases} \quad (44)$$

Substituting the element of G in Eq. (43), we can show that the largest eigenvalue of $G + G^\dagger$ is strictly negative provided the following conditions are satisfied:

$$0 \geq \begin{cases} 2j\mu(E_{1,s}) + (2j-1)\|E_{2,s}\| + (2j+1)\|E_{0,s}\| & \text{for } j = 2, \dots, N-1 \\ 2\mu(E_{1,s}) + \|E_{2,s}\| + 2\|E_{0,s}\| & \text{for } j = 1 \\ 2N\mu(E_{1,s}) + (N-1)\|E_{2,s}\| + N\|E_{0,s}\| & \text{for } j = N \end{cases} \quad (45)$$

It is sufficient to have the following conditions to ensure the above three conditions are satisfied:

$$\begin{cases} \mu(E_{1,s}) + \|E_{2,s}\| + \|E_{0,s}\| < 0 \\ 4\mu(E_{1,s}) + 3\|E_{2,s}\| + 5\|E_{0,s}\| < 0 \\ 2\mu(E_{1,s}) + \|E_{2,s}\| + 2\|E_{0,s}\| < 0. \end{cases} \quad (46)$$

The third inequality can be derived by the first two, thus

$$C_E := \max\{4\mu(E_{1,s}) + 3\|E_{2,s}\| + 5\|E_{0,s}\|, \mu(E_{1,s}) + \|E_{2,s}\| + \|E_{0,s}\|\} < 0 \Rightarrow \mu(G) \leq \frac{1}{2}C_E < 0. \quad (47)$$

We will show later that this C_E in (47) matches the C_E defined in Theorem IV.1 (33) when $Q = \sqrt{P}/\gamma$, see Eq. (60) for detail.

Now, let's assume (47) is satisfied (we will show that it can be satisfied by choosing Q properly later). Since (42) is established for any ξ , we have $\mu(B_N) \leq \mu(G)$. The forcing term \hat{d}_N can be upper bounded by Cauchy Schwartz inequality and $\|B_{N,N+1}\| = \sum_{m=1}^N \|I^{\otimes(m-1)} \otimes E_{2,s} \otimes I^{N-m}\| \leq \sum_{m=1}^N \|E_{2,s}\| = N\|E_{2,s}\|$ as

$$\xi^\dagger \hat{d}_N + \hat{d}_N^\dagger \xi = 2\text{Re}(\xi_N B_{N,N+1} v^{\otimes(N+1)}(t)) \leq 2N\|\xi\|\|E_{2,s}\|\|v(t)\|^{N+1} \quad (48)$$

Consequently, we have $\frac{d}{dt}\|\xi\|^2 \leq 2\mu(G)\|\xi\|^2 + 2N\|\xi\|\|E_{2,s}\|\|v\|^{N+1}$, it reveals that for $\|\xi\| > 0$, we have

$$\frac{d}{dt}\|\xi\| \leq \mu(G)\|\xi\| + N\|E_{2,s}\|\|v(t)\|^{N+1}, \quad \|\xi(0)\| = 0. \quad (49)$$

By Grönwall's inequality, we obtain

$$\|\xi(t)\| \leq tN\|E_{2,s}\| \max_{t \in [0,T]} \|v(t)\|^{N+1}. \quad (50)$$

Finally, when $Q = \sqrt{P}/\gamma$, we note that

$$\mu(E_{1,s}) = \mu_P(F_{1,s}), \quad \|E_{2,s}\| = \gamma\|F_{2,s}\|_P, \quad \|E_{0,s}\| = \frac{1}{\gamma}\|F_{0,s}\|_P.$$

The condition in Eq. (47) is then satisfied when $\gamma \in (\zeta_-^P, r_+^P)$. This concludes the proof of Proposition IV.3. \square

In the remaining part of this section, we will provide the proof of Lemma IV.5. We first provide a bound for general Lyapunov transformation and then show that the special case reveals the results in Lemma IV.5.

Lemma IV.6 (Stable system: long time bound of $\|v(t)\|$). *Define $O = Q^\dagger Q$, where Q is the Lyapunov transform matrix defined in Eq. (21). Suppose $\mu_O(F_{1,s}) < 0$ and $\mu_O(F_{1,s})^2 - 4\|F_{2,s}\|_O\|F_{0,s}\|_O > 0$. Consider $u(t)$ in Eq. (20) and $v(t)$ in Eq. (22). Define*

$$r_\pm^O = \frac{-\mu_O(F_{1,s}) \pm \sqrt{\mu_O(F_{1,s})^2 - 4\|F_{2,s}\|_O\|F_{0,s}\|_O}}{2\|F_{2,s}\|_O}. \quad (51)$$

Then,

- If $\|u(0)\|_O = \|v(0)\| \in [r_-^O, r_+^O)$, then $\|u(t)\|_O = \|v(t)\| \leq \|u(0)\|_O < r_+^O$.
- If $\|u(0)\|_O = \|v(0)\| \in [0, r_-^O)$, then $\|u(t)\|_O = \|v(t)\| < r_-^O$.

The proof of the solution bound follows the comparison theorem and the bound for scalar Riccati equation.

Proof of Lemma IV.6. We first estimate the time derivative of $\|v\|^2 = v^\dagger v$,

$$\begin{aligned} \partial_t \|v\|^2 &= v^\dagger E_{2,s}(v \otimes v) + (v^\dagger \otimes v^\dagger) E_{2,s}^\dagger v + v^\dagger (E_{1,s} + E_{1,s}^\dagger) v + v^\dagger E_{0,s} + E_{0,s}^\dagger v \\ &\leq 2\|E_{2,s}\|\|v\|^3 + 2\mu(E_{1,s})\|v\|^2 + 2\|E_{0,s}\|\|v\|. \end{aligned} \quad (52)$$

If $\|v\| \neq 0$, this implies

$$\partial_t \|v(t)\| \leq \|E_{2,s}\|\|v\|^2 + \mu(E_{1,s})\|v\| + \|E_{0,s}\|. \quad (53)$$

Consider the scalar comparison ODE for $z(t) = \|v(t)\|$,

$$\partial_t z = \|E_{2,s}\|z^2 + \mu(E_{1,s})z + \|E_{0,s}\| \quad (54)$$

When its discriminant is positive,

$$\Delta = \mu(E_{1,s})^2 - 4\|E_{2,s}\|\|E_{0,s}\| > 0, \quad (55)$$

the quadratic polynomial admits two distinct real roots

$$r_\pm := \frac{-\mu(E_{1,s}) \pm \sqrt{\mu(E_{1,s})^2 - 4\|E_{2,s}\|\|E_{0,s}\|}}{2\|E_{2,s}\|}. \quad (56)$$

From the relationship between $E_{i,s}$ and $F_{i,s}$ in Eq. (23) and the properties of the weighted inner product introduced in Section II, we have

$$\mu(E_{1,s}) = \mu_O(F_{1,s}), \|E_{0,s}\| = \|F_{0,s}\|_O, \|E_{2,s}\| = \|F_{2,s}\|_O, \|v(t)\| = \|u(t)\|_O. \quad (57)$$

Substituting them into the expression of r_{\pm} in Eq. (56), we can rewrite those two roots as

$$r_{\pm} = \frac{-\mu_O(F_{1,s}) \pm \sqrt{\mu_O(F_{1,s})^2 - 4\|F_{2,s}\|_O\|F_{0,s}\|_O}}{2\|F_{2,s}\|_O} = r_{\pm}^O. \quad (58)$$

By the comparison theorem, we obtain the bound on $\|v(t)\|$ and its dependence on $\|v(0)\|$, i.e.

- If $\|v(0)\| \in [r_-^O, r_+^O)$, then $\|v(t)\| \leq \|v(0)\| < r_+^O$.
- If $\|v(0)\| \in [0, r_-^O)$, then $\|v(t)\| < r_-^O$.

With $\|v(0)\| = \|u(0)\|_O$, $\|v(t)\| = \|u(t)\|_O$, this completes the proof. \square

Now, we are ready to prove Lemma IV.5 by applying Lemma IV.6 with a specific choice of Q :

Proof of Lemma IV.5. The conditions in Lemma IV.6 are satisfied by choosing $Q = \sqrt{P}/\gamma$ under Assumptions I.1 and I.2. From Assumptions I.1, we have

$$PF_{1,s} + F_{1,s}^\dagger P \prec 0.$$

From the property of log norm in Section II, the weighted log norm is negative as

$$\mu_O(F_{1,s}) = \frac{1}{2} \max_i \lambda_i \left(\sqrt{P}^{-1} \left(PF_{1,s} + F_{1,s}^\dagger P \right) \sqrt{P}^{-1} \right) < 0. \quad (59)$$

because P is hermitian. Under Assumptions I.2, we have

$$\mu_P(F_{1,s})^2 - 4\|F_{2,s}\|_P\|F_{0,s}\|_P > 0.$$

Furthermore, with $Q = \sqrt{P}/\gamma$, we have

$$\mu_O(F_{1,s}) = \mu_P(F_{1,s}), \quad \|F_{2,s}\|_O = \gamma\|F_{2,s}\|_P, \quad \|F_{0,s}\|_O = \frac{1}{\gamma}\|F_{0,s}\|_P, \quad \|v(t)\|_O = \|u(t)\|. \quad (60)$$

The first three equations in Eq. (60) imply that $\mu_O(F_{1,s})^2 - 4\|F_{2,s}\|_O\|F_{0,s}\|_O > 0$ and $r_{\pm}^O = \frac{1}{\gamma}r_{\pm}^P$. This concludes the proof of Lemma IV.5. \square

B. Quantum solvers for linear differential equations

In this section, we analyze the query complexity of the quantum algorithm applied to the linear differential equation in Eq. (24). This completes the third step of the complexity analysis. According to (42),(47),(60) in the proof of Proposition IV.3, we have

$$B_N + B_N^\dagger \leq \frac{1}{2}C_E := \frac{1}{2} \max\{4\mu_O(F_{1,s}) + 3\|F_{2,s}\|_O + 5\|F_{0,s}\|_O, \mu_O(F_{1,s}) + \|F_{2,s}\|_O + \|F_{0,s}\|_O\} < 0$$

under the assumption of Theorem IV.1. By applying the quantum algorithm [45] for dissipative differential equations, we obtain the following result for solving the Carleman linearized system.

Proposition IV.7 (Stable system). *Under the assumption of Theorem IV.1. Let $\epsilon > 0$ and assume the simulation time $T \geq 1/|C_E|$. There exists a quantum algorithm that outputs an ϵ -approximation of the final state $|v(T)\rangle$ using*

$$\tilde{O} \left(\frac{\sqrt{T}g_v}{\sqrt{|C_E|}} \alpha_E \text{poly} \log(1/\epsilon) \right) \quad (61)$$

queries to the block-encoding of $F_{i,s}$, for $i = 0, 1, 2$, and the state preparation oracle of $|v(0)\rangle$,

$$\tilde{O} \left(\frac{\kappa_Q^2 \sqrt{T}g_v}{\sqrt{|C_E|}} \alpha_E \text{poly} \log(1/\epsilon) \right) \quad (62)$$

queries to the block-encoding of Q . Here α_E, g_v are defined in Section IA, κ_Q is the condition number of $Q := \sqrt{P}/\gamma$ defined in Theorem IV.1.

In general, the shifted system may remain unstable even after pivot shift. Nevertheless, over a short time interval, one can still establish the following query complexity using the quantum algorithm for linear differential equations [28].

Proposition IV.8 (Unstable system). *Under the assumption of Theorem IV.2, we choose t^* as in Proposition IV.4. For any $T \leq t^*$, there exists a quantum algorithm to solve the quadratic ODE and output a quantum state ϵ -close to the final state $|v(T)\rangle$ using*

$$\tilde{\mathcal{O}} \left(g_v \frac{(\alpha_{F_{0,s}} + \alpha_{F_{1,s}} + \alpha_{F_{2,s}}) \|F_{2,s}\| T^2}{\|v(T)\| \epsilon} \text{poly log}(n) \right) \quad (63)$$

queries to the block-encoding of $F_{i,s}$. Here, $\alpha_{F_{i,s}}$ is the block-encoding factor for $F_{i,s}$, defined in Lemma II.4.

We put the proof of Proposition IV.8 in Section B.

Before proving Proposition IV.7, we quantify the normalizing coefficient for B_N and d_N in Eq. (24). Follows the argument in [27, (L.3)-(L.6)], we have

- $\alpha_{d_N} = \|E_{0,s}\| = \alpha_{F_{0,s}} \alpha_Q$,
- $\alpha_{B_N} = N(\alpha_{F_{0,s}} \alpha_Q + \alpha_{F_{1,s}} \kappa_Q + \frac{\alpha_{F_{2,s}} \kappa_Q^2}{\alpha_Q})$.

By LCU and quantum singular value transformation [3], a single query to the block encoding oracle of B_N requires one call to each block encoding of $F_{i,s}$, $i = 0, 1, 2$ and $\mathcal{O}(\kappa_Q^2 \log(1/\epsilon)^2)$ calls to the block encoding of Q with precision ϵ . Moreover, one query to the state preparation oracle for $|d_N\rangle$ requires one call to $E_{0,s}$ and one call to the block encoding of Q . From [26, Lemma 5], the initial state $\hat{z}(0)$ can be prepared with N queries to the state preparation oracle for $|v(0)\rangle$.

Proof of Proposition IV.7. The complexity of QLSA based Carleman linearization method can be obtained by applying QLSA in Corollary 12 in [45]. We first state the result here.

Lemma IV.9. *(The time independent version for final state preparation in [45, Corollary 12]) Using the truncated Taylor series method for solving the ODEs $\partial_t u = Au + b$, $t \in [0, T]$ with initial condition $u(0) = u_0$. Suppose the A is a matrix such that $A + A^\dagger \leq -2\eta < 0$. Let $\epsilon > 0$ be the target error, $T \geq \eta^{-1}$ be the evolution time, α_A be the block-encoding factor of A and α_b be the normalization factor of b . Then we can obtain an ϵ -approximation of the final state $u(T)/\|u(T)\|$ using*

$$\tilde{\mathcal{O}} \left(\frac{\max_t \|u(t)\|}{\|u(T)\|} \frac{\alpha_A \sqrt{T}}{\sqrt{\eta}} \log \left(\frac{\|u_0\| + \alpha_b \alpha_A}{\|u(T)\| \eta \epsilon} \right) \log \left(\frac{1}{\epsilon} \right) \right) \quad (64)$$

queries to the block encoding of A and

$$\tilde{\mathcal{O}} \left(\frac{\max_t \|u(t)\|}{\|u(T)\|} \frac{\alpha_A \sqrt{T}}{\sqrt{\eta}} \log \left(\frac{1}{\epsilon} \right) \right) \quad (65)$$

queries to the state preparation of $|u_0\rangle$ and $|b\rangle$.

In our setting, we first apply the above lemma to solve the Carleman linearized equation $\partial_t \hat{z} = B_N \hat{z} + d_N$ and then calculate the extra rounds from amplitude amplification to extract the approximation of $v(T)$. We denote the quantum state after applying the QLSA as \tilde{z} then the first block \tilde{z}_1 , the same block when Carleman truncation order $N = 1$, approximates $v(T)$. First, we denote the precision from QLSA as ϵ' . For all $\epsilon' > 0$ and $T \geq 1/|C_E|$,

$$\left\| \tilde{z} - \frac{\hat{z}(T)}{\|\hat{z}(T)\|} \right\| \leq \epsilon' \quad (66)$$

with

$$\tilde{\mathcal{O}} \left(\frac{\max \|\hat{z}(t)\|}{\|\hat{z}(T)\|} \frac{\alpha_{B_N} \sqrt{T}}{\sqrt{|C_E|}} \log \left(\frac{\|\hat{z}(0)\| + \alpha_{d_N}}{\|\hat{z}(T)\| |C_E| \epsilon'} \right) \log(1/\epsilon') \right) \quad (67)$$

queries to block-encoding of B_N and

$$\tilde{\mathcal{O}} \left(\frac{\max_t \|\hat{z}(t)\|}{\|\hat{z}(T)\|} \frac{\alpha_{B_N} \sqrt{T}}{\sqrt{|C_E|}} \log(1/\epsilon') \right) \quad (68)$$

queries to the state preparation oracle of $|\hat{z}(0)\rangle$ and $|d_N\rangle$. Let the Carleman linearization error bounded by δ' . Proposition IV.3 shows that $\|\xi_j(T)\| \leq \|\xi(T)\| \leq \delta' \|v(T)\|$ can be achieved with truncation order $N \geq \log(T\|E_{2,s}\|/\delta'\|v(T)\|)/\log(1/\max_{t \in [0,T]} \|v(t)\|)$.

Through measuring the quantum registers, we use the first block, \tilde{z}_1 , of size corresponding to Carlman linearization truncated at $N = 1$, to approximate $v(T)$. The success probability can be approximated as

$$\begin{aligned} \|\tilde{z}_1\| &\geq \frac{\|\hat{z}_1(T)\|}{\|\hat{z}(T)\|} - \left\| \frac{\hat{z}_1(T)}{\|\hat{z}(T)\|} - \tilde{z}_1 \right\| \\ &\geq \frac{\|\hat{z}_1(T)\|}{\|\hat{z}(T)\|} - \left\| \frac{\hat{z}(T)}{\|\hat{z}(T)\|} - \tilde{z} \right\| \geq \frac{\|\hat{z}_1(T)\|}{\|\hat{z}(T)\|} - \epsilon'. \end{aligned} \quad (69)$$

With $\max_{t \in [0,T]} \|v(t)\| \leq 1$, the upper and lower bounds of \hat{z} can be analyzed similar to the technique in [28, Theorem 8]

- $\|\hat{z}(T)\| \geq \|\hat{z}_1(T)\| \geq \|v(T)\| - \|v(T) - \hat{z}_1(T)\| \geq \|v(T)\|(1 - \delta')$,
- $\|\hat{z}(T)\| \leq \sqrt{N}(1 + \delta')\|v(T)\|$,
- $\frac{\|\hat{z}_1(T)\|}{\|\hat{z}(T)\|} \geq \frac{(1-\delta')\|v(T)\|}{\sqrt{N}(1+\delta')\|v(T)\|} = \frac{(1-\delta')}{\sqrt{N}(1+\delta')}$.

Therefore, we have $\|\tilde{z}_1\| \geq \frac{(1-\delta')}{\sqrt{N}(1+\delta')} - \epsilon'$ and

$$\frac{\max_t \|\hat{z}(t)\|}{\|\hat{z}(T)\|} \leq \frac{\sqrt{N}(1 + \delta') \max_{t \in [0,T]} \|v(t)\|}{(1 - \delta')\|v(T)\|} = \sqrt{N} \frac{1 + \delta'}{1 - \delta'} g_v, \quad \|\hat{z}(0)\| \leq \sqrt{N}(1 + \delta')\|v(0)\|. \quad (70)$$

By choosing $\epsilon' = \Theta\left(\frac{\epsilon}{\sqrt{N}}\right)$, $\delta' = \Theta(\epsilon)$, the success probability in Eq. (69) is lower bounded by $\Theta(1/N)$, it can be boosted to a constant using $\mathcal{O}(\sqrt{N})$ rounds of amplitude amplification.

To bound the approximation error from \tilde{z}_1 , we use

$$\begin{aligned} \left\| \frac{\tilde{z}_1}{\|\tilde{z}_1\|} - \frac{v(T)}{\|v(T)\|} \right\| &\leq \left\| \frac{\tilde{z}_1}{\|\tilde{z}_1\|} - \frac{\hat{z}_1(T)/\|\hat{z}(T)\|}{\|\hat{z}_1(T)\|/\|\hat{z}(T)\|} \right\| + \left\| \frac{\hat{z}_1(T)}{\|\hat{z}_1(T)\|} - \frac{v(T)}{\|v(T)\|} \right\| \\ &\leq 2 \frac{\left\| \tilde{z}_1 - \frac{\hat{z}_1(T)}{\|\hat{z}(T)\|} \right\|}{\|\tilde{z}_1\|} + \left\| \frac{\hat{z}_1(T)}{\|\hat{z}_1(T)\|} - \frac{v(T)}{\|v(T)\|} \right\| \leq \frac{2\epsilon'}{\|\tilde{z}_1\|} + \frac{2\|v(T) - \hat{z}_1(T)\|}{\|v(T)\|} \leq \frac{2\epsilon'}{\|\tilde{z}_1\|} + 2\delta'. \end{aligned} \quad (71)$$

Still by choosing $\epsilon' = \Theta\left(\frac{\epsilon}{\sqrt{N}}\right)$, $\delta' = \Theta(\epsilon)$, the above error $\left\| \frac{\tilde{z}_1}{\|\tilde{z}_1\|} - \frac{v(T)}{\|v(T)\|} \right\|$ can be bounded by $\mathcal{O}(\epsilon)$.

Combining the QLSA complexity with the amplitude amplification overhead yields

$$\begin{aligned} &\tilde{\mathcal{O}} \left(\underbrace{\frac{\max_t \|\hat{z}(t)\|}{\|\hat{z}(T)\|} \frac{\alpha_{B_N} \sqrt{T}}{\sqrt{|C_E|}} \log \left(\frac{\|\hat{z}(0)\| + \alpha_{d_N} \frac{\alpha_{B_N}}{|C_E|} \epsilon'}{\|\hat{z}(T)\|} \right) \log(1/\epsilon') \times \sqrt{N}}_{\text{From (67)}} \right) \underbrace{\hspace{10em}}_{\text{Amplitude amplification}} \\ &= \mathcal{O} \left(N^2 \left(\alpha_{F_{0,s}} \alpha_Q + \alpha_{F_{1,s}} \kappa_Q + \frac{\alpha_{F_{2,s}} \kappa_Q^2}{\alpha_Q} \right) g_v \frac{\sqrt{T}}{\sqrt{|C_E|}} \right) \\ &\quad \times \log \left(\frac{3\sqrt{N}\|v(0)\| + \|E_{0,s}\|}{\|v(T)\|} \frac{N^{3/2} g_v \left(\alpha_{F_{0,s}} \alpha_Q + \alpha_{F_{1,s}} \kappa_Q + \frac{\alpha_{F_{2,s}} \kappa_Q^2}{\alpha_Q} \right)}{|C_E| \epsilon} \right) \log(\sqrt{N}/\epsilon) \end{aligned} \quad (72)$$

queries to the block-encodings of $F_{i,s}$, $i = 0, 1, 2$,

$$\mathcal{O} \left(N^2 \left(\alpha_{F_{0,s}} \alpha_Q + \alpha_{F_{1,s}} \kappa_Q + \frac{\alpha_{F_{2,s}} \kappa_Q^2}{\alpha_Q} \right) g_v \frac{\sqrt{T}}{\sqrt{|C_E|}} \log(\sqrt{N}/\epsilon) \right) \quad (73)$$

queries to the state preparation oracle of $|v(0)\rangle$ and $|d_N\rangle$.

In the equality, we use (70), the definition of α_{B_N} and α_{d_N} , and the choice of ϵ' . Plugging in the dependence of N , up to polylogarithmic factors, the calls to coefficient matrices $F_{i,s}$, $i = 0, 1, 2$ become

$$\tilde{\mathcal{O}}\left(\sqrt{T} \frac{g_v}{\sqrt{|C_E|}} \left(\alpha_{F_{0,s}} \alpha_Q + \alpha_{F_{1,s}} \kappa_Q + \frac{\alpha_{F_{2,s}} \kappa_Q^2}{\alpha_Q} \right) \text{polylog}(T/\epsilon)\right). \quad (74)$$

Since one query of B_N requires $\mathcal{O}(\kappa_Q^2 \log(1/\epsilon)^2)$ calls to the block encoding of Q , the number of queries to the block-encoding of Q is

$$\tilde{\mathcal{O}}\left(\kappa_Q^2 \sqrt{T} \frac{g_v}{\sqrt{|C_E|}} \left(\alpha_{F_{0,s}} \alpha_Q + \alpha_{F_{1,s}} \kappa_Q + \frac{\alpha_{F_{2,s}} \kappa_Q^2}{\alpha_Q} \right) \text{polylog}(T/\epsilon)\right), \quad (75)$$

and the number of queries to the state-preparation oracle for $|v(0)\rangle$ is

$$\tilde{\mathcal{O}}\left(\sqrt{T} \frac{g_v}{\sqrt{|C_E|}} \left(\alpha_{F_{0,s}} \alpha_Q + \alpha_{F_{1,s}} \kappa_Q + \frac{\alpha_{F_{2,s}} \kappa_Q^2}{\alpha_Q} \right) \text{polylog}(T/\epsilon)\right). \quad (76)$$

Plugging in the dependence of $\alpha_{F_{i,s}}$ in terms of α_{F_i} and α_Q from Lemma II.4, we conclude the proof. \square

C. Proof of the main theorem

In this section, we combine the results from the previous sections to prove the main theorem for stable systems, i.e. Theorem IV.1. The proof of the main theorem for unstable systems, i.e. Theorem IV.2, is given in Section B.

Proof of Theorem IV.1. By applying quantum solvers to the Carleman linearized differential equation, there exists quantum algorithm that outputs the ϵ' -approximation of the final state, $|\hat{v}_T\rangle$, so that

$$\left\| |\hat{v}_T\rangle - \frac{v(T)}{\|v(T)\|} \right\| \leq \epsilon'. \quad (77)$$

From Proposition IV.7, we obtain the query complexity in terms of $\alpha_{F_{i,s}}$, g_v and the state preparation oracle of $|v(0)\rangle$. Recall that Q is block-encoded with factor $\alpha_Q = \mathcal{O}(\|Q\|)$. We then apply Lemma II.3 with $A = Q/\alpha_Q$, the state $|Q^{-1}\hat{v}_T\rangle$ with precision ϵ'' can be produced with $\mathcal{O}(\kappa_Q \log(1/\epsilon''))$ calls to the oracle for $|\hat{v}_T\rangle$ and Q . We denote the state as $|\hat{u}_T\rangle$, then

$$\left\| |\hat{u}_T\rangle - \frac{Q^{-1}\hat{v}_T}{\|Q^{-1}\hat{v}_T\|} \right\| \leq \epsilon''. \quad (78)$$

Combining the error from the quantum algorithm for linearized equation and the inverse matrix multiplication, we have

$$\begin{aligned} & \left\| |\hat{u}_T\rangle - \frac{u(T)}{\|u(T)\|} \right\| \\ & \leq \left\| |\hat{u}_T\rangle - \frac{Q^{-1}\hat{v}_T}{\|Q^{-1}\hat{v}_T\|} \right\| + \left\| \frac{Q^{-1}\hat{v}_T}{\|Q^{-1}\hat{v}_T\|} - \frac{Q^{-1}v(T)}{\|Q^{-1}v(T)\|} \right\| \\ & \leq \left\| |\hat{u}_T\rangle - \frac{Q^{-1}\hat{v}_T}{\|Q^{-1}\hat{v}_T\|} \right\| + \|Q^{-1}\| \left\| \frac{\hat{v}_T/\|\hat{v}_T\|}{\|Q^{-1}\hat{v}_T\|/\|\hat{v}_T\|} - \frac{v(T)/\|v(T)\|}{\|Q^{-1}v(T)\|/\|v(T)\|} \right\| \\ & \leq \epsilon'' + \|Q^{-1}\| \frac{2\|v(T)\|}{\|u(T)\|} \left\| \frac{\hat{v}_T}{\|\hat{v}_T\|} - \frac{v(T)}{\|v(T)\|} \right\| \leq \epsilon'' + 2\kappa_Q \epsilon' \end{aligned} \quad (79)$$

We choose $\epsilon' = \epsilon/(4\kappa_Q)$ and $\epsilon'' = \epsilon/2$, according to Proposition IV.7, there exists a quantum algorithm that output the state approximate $|u(T)\rangle$ up to ϵ using

$$\tilde{\mathcal{O}}\left(\frac{\kappa_Q \sqrt{T} g_v}{\sqrt{|C_E|}} \alpha_E \text{polylog}(4\kappa_Q/\epsilon)\right) \quad (80)$$

queries to the block-encoding of $F_{i,s}$, for $i = 0, 1, 2$, and the state preparation oracle of $|v(0)\rangle$,

$$\tilde{\mathcal{O}} \left(\frac{\kappa_Q^3 \sqrt{T} g_v}{\sqrt{|C_E|}} \alpha_E \text{poly log}(4\kappa_Q/\epsilon) \right) \quad (81)$$

queries to the block-encoding of Q .

Finally, we use the final state shift oracle in Lemma II.4. We first note that the success probability $p = \Theta(1)$ after amplitude amplification. The final state $|x(T)\rangle$ can be obtained from

$$\mathcal{O} \left(\frac{\sqrt{\|x(T) - s\|^2 + \|s\|^2}}{\|x(T)\|} \right) \quad (82)$$

queries to the state preparation oracle of $|u(T)\rangle$ and O_s .

Combining it with the initial state shift oracle in Lemma II.4, we note that we need $\mathcal{O} \left(\frac{\sqrt{\|x(0)\|^2 + \|s\|^2}}{\|x(0) - s\|} \right)$ queries to O_{x_0} and O_s for preparing $U_{|u(0)\rangle}$ and $\mathcal{O}(\kappa_Q)$ queries to $U_{|v(0)\rangle}$ for preparing $U_{|v(0)\rangle}$, there exist a quantum algorithm that approximate the final state $|x(T)\rangle$ up to precision ϵ using

$$\tilde{\mathcal{O}} \left(\frac{\sqrt{\|x(T) - s\|^2 + \|s\|^2}}{\|x(T)\|} \frac{\kappa_Q \sqrt{T} g_v}{\sqrt{|C_E|}} \alpha_E \text{poly log}(4\kappa_Q/\epsilon) \right) \quad (83)$$

queries to the block-encoding of O_{F_i} for $i = 0, 1, 2$, and

$$\tilde{\mathcal{O}} \left(\frac{\sqrt{\|x(T) - s\|^2 + \|s\|^2}}{\|x(T)\|} \frac{\sqrt{\|x(0)\|^2 + \|s\|^2}}{\|x(0) - s\|} \frac{\kappa_Q^2 \sqrt{T} g_v}{\sqrt{|C_E|}} \alpha_E \text{poly log}(4\kappa_Q/\epsilon) \right) \quad (84)$$

queries to O_{x_0} and O_s ,

$$\tilde{\mathcal{O}} \left(\frac{\sqrt{\|x(T) - s\|^2 + \|s\|^2}}{\|x(T)\|} \frac{\kappa_Q^3 \sqrt{T} g_v}{\sqrt{|C_E|}} \alpha_E \text{poly log}(4\kappa_Q/\epsilon) \right) \quad (85)$$

queries to the block-encoding of Q . This concludes the proof of Theorem IV.1. \square

The analysis for unstable systems follow the same idea and is postponed to Section B.

V. NUMERICAL TESTS

We evaluate the proposed pivot-shifted Carleman (PSC) method on two canonical nonlinear systems: the 1D logistic equation and the 2D Lotka–Volterra predator-prey equations. For each system, we assess solution accuracy by computing the ℓ_2 norm of the error between the simulated trajectory and a reference benchmark. For the logistic equation, the benchmark is the closed-form analytical solution; for the Lotka–Volterra system, it is a high-order Runge–Kutta solution. Both the standard Carleman linearization and the PSC variant are evaluated against these benchmarks to quantify the accuracy gain afforded by the pivot shift. The source code is available in our GitHub repository [50].

A. Logistic equation

We begin with the logistic equation, where x is a scalar variable:

$$\frac{dx}{dt} = x(1 - x), \quad x(0) = x_0. \quad (86)$$

We set $x_0 = 0.5$ and evaluate both the standard Carleman linearization and the PSC method over $[0, 10]$ across a range of truncation orders. Figure 2(a)–(d) display the solution trajectories and pointwise errors at $N = 4$ and $N = 8$.

The Carleman solution is unstable and diverges substantially from the analytical solution, as seen in Fig. 2(a) and (c). This is because the logistic equation, when cast in the form of Eq. (1), yields $\alpha(F_1) = 1 > 0$, violating the stability

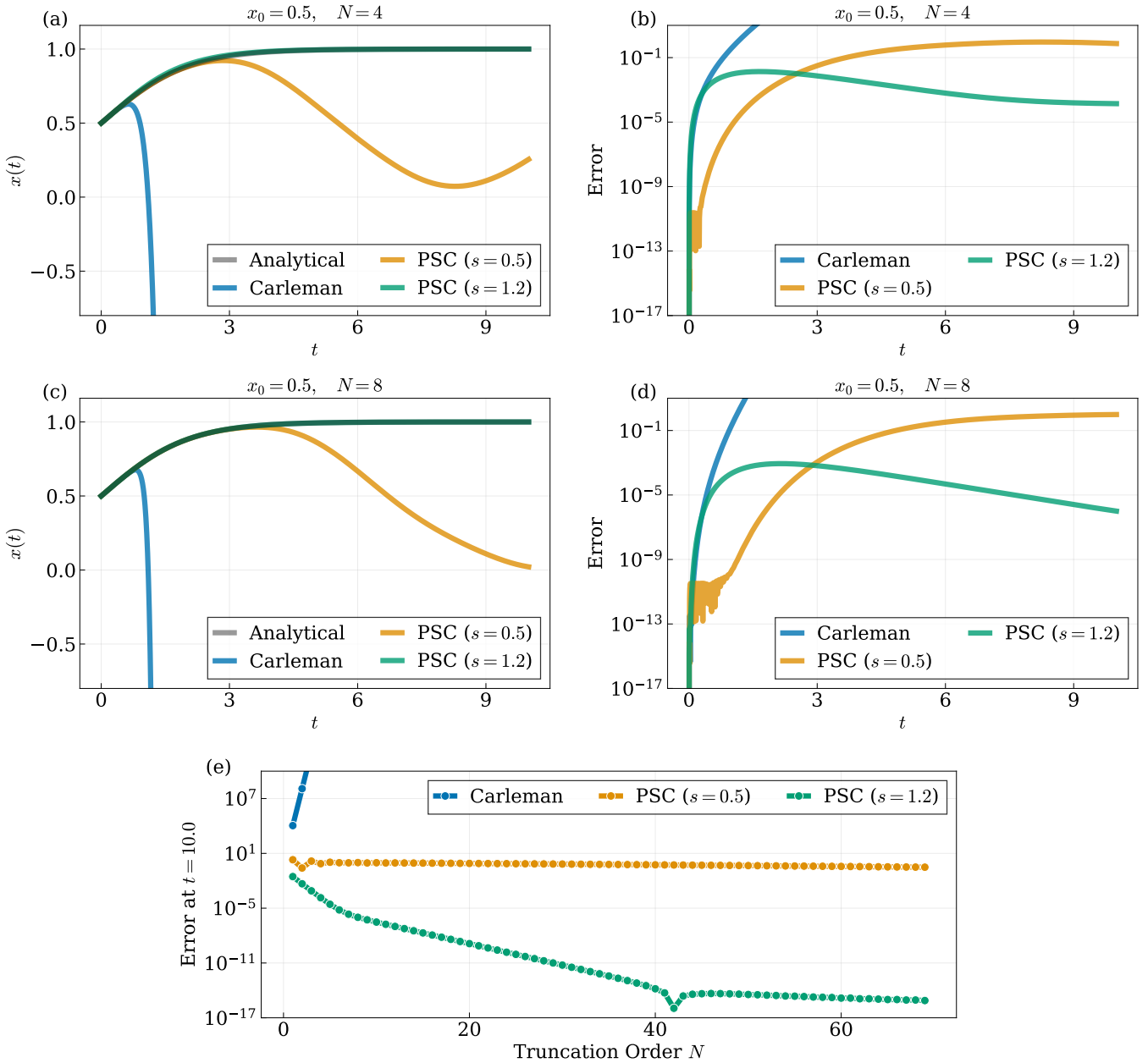


Figure 2: Performance of the standard Carleman linearization and the PSC method on the logistic equation Eq. (86) with $x_0 = 0.5$. (a), (c): Solution trajectories of the exact solution, Carleman, PSC with $s = 0.5$, and PSC with $s = 1.2$, at truncation orders $N = 4$ and $N = 8$, respectively. (b), (d): Corresponding pointwise errors on a semi-logarithmic scale. The standard Carleman method diverges in both cases due to the violated stability condition $\alpha(F_1) = 1 > 0$. The PSC method with $s = 0.5$ also eventually diverges, as this pivot s lies outside the admissible region. The PSC method with $s = 1.2$ remains stable and achieves substantially lower error. (e): Error at the final time $t = 10$ as a function of truncation order $N \in [1, 69]$. While the errors of Carleman and PSC with $s = 0.5$ stagnate or grow with N , PSC with $s = 1.2$ exhibits exponential convergence, confirming the theoretical analysis.

condition in Assumption I.1. Consequently, the Carleman solution departs from the exact solution at approximately $t = 1.2$.

The PSC method addresses this instability by introducing the shifted variable $u = x - s$ and applying Carleman linearization to the resulting system. Rewriting the logistic equation in the form of Eqs. (19) and (20) gives

$$\frac{du}{dt} = -u^2 + (1 - 2s)u + s - s^2, \quad u(0) = u_0 := x_0 - s, \quad (87)$$

with coefficients $F_{2,s} = -1$, $F_{1,s} = 1 - 2s$, and $F_{0,s} = s - s^2$. The stability condition Assumption I.1 then requires

$$\alpha(F_{1,s}) = \mu(F_{1,s}) = 1 - 2s < 0, \quad (88)$$

i.e., $s > 1/2$. We test two pivots, $s = 0.5$ and $s = 1.2$, to illustrate this dependence. When $s = 0.5$, the stability condition is marginally violated and the PSC solution is expected to diverge over time. Fig. 2(a) and (c) confirm this: at $N = 4$ and $N = 8$, the PSC trajectory begins to deviate near $t = 3$, and the error plots in Fig. 2(b) and (d) quantify the rapid error growth for long time evolution. Fig. 2(e) reinforces this further, showing that the error of PSC with $s = 0.5$ stagnates as N increases, with no meaningful improvement from higher truncation orders.

In contrast, when the pivot is chosen near the stable equilibrium $x^* = 1$, exemplified by $s = 1.2$, the PSC solution closely tracks the analytical solution throughout the entire time interval. Fig. 2(a) and (c) show that the trajectory remains accurate at both truncation orders, and the error plots in Fig. 2(b) and (d) confirm that the error stays consistently low, in the range of 10^{-3} to 10^{-5} . Fig. 2(e) further demonstrates the advantage of this pivot choice: the error at $s = 1.2$ decays exponentially with N , confirming that proximity to the stable equilibrium is the key criterion for selecting an effective pivot. The comparison between $s = 0.5$ and $s = 1.2$ highlights the importance of choosing a correct pivot for the PSC method. The former, although closer to the initial condition, fails to achieve high accuracy due to the violation of the stability condition, while the latter, despite being farther from the initial condition, successfully stabilizes the solution and achieves exponential convergence.

B. Lotka-Volterra equations

We now test Carleman and PSC methods on a two-dimensional Lotka-Volterra predator-prey model as presented in [39, Equation 37],

$$\begin{aligned} \partial_t x_1 &= \eta x_1 - \beta x_1 x_2, \\ \partial_t x_2 &= -\gamma x_2 + \delta x_1 x_2, \end{aligned}$$

where $\eta, \gamma, \beta, \delta > 0$. The system can be reduced in two parameters by normalizing x_1 and x_2

$$\begin{aligned} \partial_t x_1 &= \eta x_1 - \eta x_1 x_2, \\ \partial_t x_2 &= -\gamma x_2 + \gamma x_1 x_2, \end{aligned} \quad (89)$$

where $\eta, \gamma > 0$. The system admits two unstable equilibrium points, $(0, 0)$ and $(1, 1)$ (Specifically, $(1, 1)$ does not satisfy Assumption I.1 but is Lyapunov stable).

Let the vector $x = (x_1, x_2)^\top$. Then Eq. (89) can be rewritten in the form of Eq. (1) with

$$F_0 = 0, \quad F_1 = \begin{pmatrix} \eta & 0 \\ 0 & -\gamma \end{pmatrix}, \quad F_2 = \begin{pmatrix} 0 & -\eta & 0 & 0 \\ 0 & \gamma & 0 & 0 \end{pmatrix}. \quad (90)$$

Since $\alpha(F_1) = \eta > 0$, the Lotka-Volterra equations provide an example of an unstable ordinary differential equation for which the Carleman algorithm diverges in finite time interval $[0, T]$, where the end time $T < t^*$, in accordance with Lemma B.1 and Proposition IV.4.

In the PSC method, we introduce the shifted variable $u = x - s$, then the coefficients in Eq. (20) are

$$F_{1,s} = \begin{pmatrix} \eta - \eta s_2 & -\eta s_1 \\ \gamma s_2 & -\gamma + \gamma s_1 \end{pmatrix}, \quad F_{0,s} = \begin{pmatrix} \eta(s_1 - s_1 s_2) \\ \gamma(s_1 s_2 - s_2) \end{pmatrix}. \quad (91)$$

For pivot choice $s = x(0)$, the shifted coefficient matrix $F_{1,s}$ becomes the Jacobian matrix at the initial time point, this gives that

$$\|F_{1,s}\| \leq \sqrt{\frac{\tau + \sqrt{\tau^2 - 4\eta^2\gamma^2(s_1 + s_2 - 1)^2}}{2}} \leq \sqrt{\tau}, \quad \|F_2\| = \sqrt{\eta^2 + \gamma^2}, \quad \|F_{0,s}\| \leq \sqrt{2(\eta^2 + \gamma^2)} \quad (92)$$

where $\tau = \eta^2((1 - s_2)^2 + s_1^2) + \gamma^2(s_2^2 + (s_1 - 1)^2) \leq 2(\eta^2 + \gamma^2)$. Hence, the time limit t^* in Lemma B.1 and Proposition IV.4 can be estimated as

$$t^* \geq \frac{1}{e(1 + 2\sqrt{2})\sqrt{\eta^2 + \gamma^2}}. \quad (93)$$

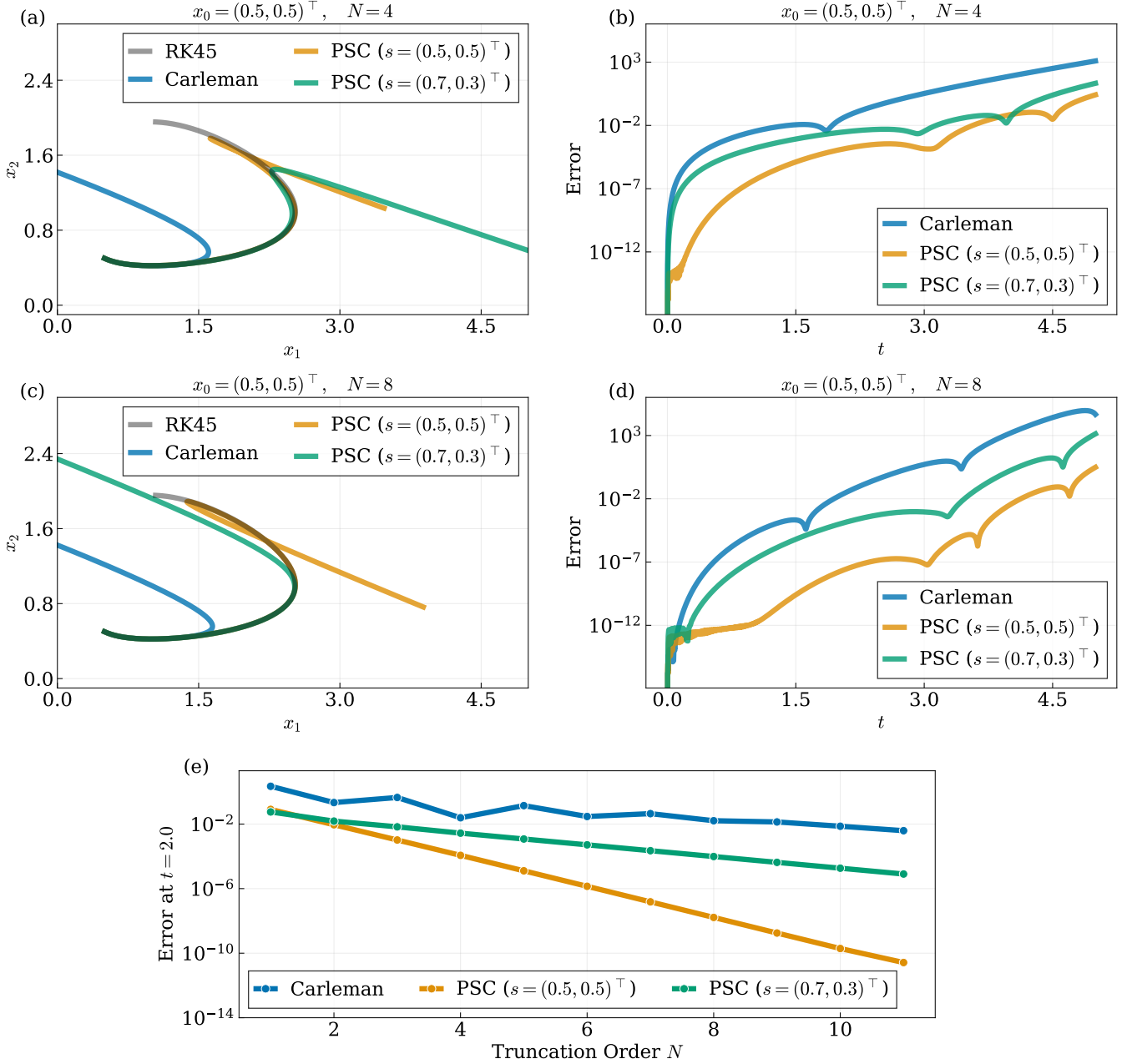


Figure 3: Performance of the standard Carleman linearization and the PSC method on the Lotka-Volterra equations with $x_0 = (0.5, 0.5)^\top$, $\eta = 1.0$, and $\gamma = 0.475$. The benchmark solution is obtained via the RK45 solver. (a), (c): Phase-plane trajectories of the benchmark solution, Carleman, PSC with $s = (0.5, 0.5)^\top$, and PSC with $s = (0.7, 0.3)^\top$, at truncation orders $N = 4$ and $N = 8$, respectively. (b), (d): Corresponding ℓ_2 norm errors over $t \in [0, 5]$ on a semi-logarithmic scale. The standard Carleman method diverges from the reference trajectory, while the PSC method remains stable; in particular, $s = (0.5, 0.5)^\top$ achieves substantially lower error at both truncation orders. (e): ℓ_2 norm error at the final time $t = 2.0$ as a function of truncation order $N \in [1, 11]$. The Carleman error stagnates or grows with N , whereas PSC converges consistently as N increases; the pivot $s = (0.5, 0.5)^\top$ yields a faster decay rate, as expected.

The simulation results for the Lotka-Volterra system are shown in Fig. 3, with parameters $\eta = 1$ and $\gamma = 0.475$. We set the initial condition $x_0 = (0.5, 0.5)^\top$ and evaluate the standard Carleman linearization and the PSC method over $t \in [0, 5]$ for two pivot choices, $s = (0.5, 0.5)^\top$ and $s = (0.7, 0.3)^\top$.

Fig. 3(a) and (b) show the phase-plane trajectories and ℓ_2 state errors at truncation order $N = 4$. The standard Carleman approximation initially tracks the reference trajectory but diverges after a short time. The PSC method

mitigates this instability for both pivots, though the degree of improvement depends on the pivot choice. With $s = (0.7, 0.3)^\top$, the PSC trajectory remains closer to the reference than Carleman but still deviates over time. With $s = (0.5, 0.5)^\top$, the trajectory follows the reference for longer and the error grows more slowly, making it the more effective pivot in this setting. This behavior is consistent with Lemma B.1 and Proposition IV.4: for both pivot choices, the linearized coefficient matrix satisfies $\alpha(F_{1,s}) > 0$, so the stability condition is violated and eventual divergence is expected for both. Nevertheless, both PSC variants substantially outperform the standard Carleman method. Fig. 3(c) and (d) display the corresponding results at $N = 8$ and exhibit the same qualitative behavior.

Fig. 3(e) complements this picture by reporting the ℓ_2 error at $t = 2$ as a function of truncation order $N \in [1, 11]$. The standard Carleman method stagnates at small N and fails to benefit from higher-order truncations. For the PSC method, the error can still be reduced by increasing N even when the stability condition is violated, provided the pivot is chosen appropriately and the evolution time is not too long. With $s = (0.5, 0.5)^\top$, the error decays rapidly with N , demonstrating that increasing the truncation order systematically improves accuracy at this time horizon. The pivot $s = (0.7, 0.3)^\top$ also yields monotone decay but at a slower rate, further confirming that $s = (0.5, 0.5)^\top$ is the more suitable pivot for this system.

VI. DISCUSSIONS AND OPEN QUESTIONS

In this work, we proposed and analyzed a pivot-shifted Carleman (PSC) method for stabilizing Carleman linearization in the solution of nonlinear ordinary differential equations. We established theoretical guarantees for the stability and convergence of the PSC method and demonstrated its effectiveness through numerical examples. Our results reveal two complementary aspects of the method. First, for stable systems, when the pivot point is chosen appropriately, the PSC method can efficiently stabilize the original Carleman linearization and achieve exponential convergence with respect to the truncation order. This modification significantly broadens the regime in which Carleman-based quantum algorithms can be applied efficiently. Second, for unstable systems, even when the stability condition is violated, we choose the pivot to be the initial condition, $s = x(0)$, so that the shifted variable satisfies $u(0) = 0$. This shrinks the standard Carleman truncation factor $\|u\|^{N+1}$ near the initial time and yields improved short-time accuracy over standard Carleman linearization, with the error continuing to decrease as the truncation order grows. This suggests that the PSC method can be beneficial even when the stability condition is not strictly satisfied or when no prior knowledge of a stable equilibrium is available. These convergence properties also provide a theoretical foundation for the single-pivot step underlying the empirical schemes in [38, 39].

There are several open questions and future directions arising from our work. First, although we have established the stability and convergence of the PSC method, the optimal choice of pivot point remains open. Developing systematic methods for selecting pivots that maximize stability and improve convergence would be valuable. Second, while our analysis focuses on quadratic nonlinearities, extending the PSC method to higher-order nonlinearities and more general classes of systems is straightforward at the algorithmic level. However, the corresponding stability and convergence analysis in these more complex settings may require new techniques and insights. Third, in the unstable case, our results show that the PSC method can achieve short time accuracy even when the stability condition is violated. As demonstrated in [39], long time simulation may also be possible by switching pivots multiple times. However, to the best of our knowledge, it remains unclear how to implement multiple pivot switching efficiently in practice, and the stability and convergence properties of such an approach are not yet well understood. Our work opens the door to addressing these questions and further advancing the theory and applications of Carleman linearization in both classical and quantum settings.

ACKNOWLEDGEMENTS

This work was supported in part by the University of Michigan through a startup grant of Z.D. (Z.D., K.W.) and the Van Loo Postdoctoral Fellowship (K.W.).

-
- [1] Richard P Feynman. Quantum mechanical computers. *Foundations of physics*, 16(6):507–531, 1986.
 - [2] Guang Hao Low and Isaac L Chuang. Hamiltonian simulation by qubitization. *Quantum*, 3:163, 2019.
 - [3] András Gilyén, Yuan Su, Guang Hao Low, and Nathan Wiebe. Quantum singular value transformation and beyond: exponential improvements for quantum matrix arithmetics. In *Proceedings of the 51st annual ACM SIGACT symposium on theory of computing*, pages 193–204, 2019.

- [4] Richard Cleve and Chunhao Wang. Efficient Quantum Algorithms for Simulating Lindblad Evolution. In *44th International Colloquium on Automata, Languages, and Programming (ICALP 2017)*, volume 80, pages 17:1–17:14. Schloss Dagstuhl – Leibniz-Zentrum für Informatik, 2017.
- [5] Xiantao Li and Chunhao Wang. Simulating Markovian Open Quantum Systems Using Higher-Order Series Expansion. In *50th International Colloquium on Automata, Languages, and Programming (ICALP 2023)*, volume 261 of *Leibniz International Proceedings in Informatics (LIPIcs)*, pages 87:1–87:20, Dagstuhl, Germany, 2023. Schloss Dagstuhl – Leibniz-Zentrum für Informatik.
- [6] Zhiyan Ding, Xiantao Li, and Lin Lin. Simulating open quantum systems using Hamiltonian simulations. *PRX quantum*, 5(2):020332, 2024.
- [7] Lin Lin and Nathan Wiebe. Quantum algorithms for scientific computation, April 2026.
- [8] Alexander M Dalzell, Sam McArdle, Mario Berta, Przemyslaw Bienias, Chi-Fang Chen, András Gilyén, Connor T Hann, Michael J Kastoryano, Emil T Khabiboulline, Aleksander Kubica, et al. *Quantum algorithms: A survey of applications and end-to-end complexities*. Cambridge University Press, 2025.
- [9] Aram W Harrow, Avinandan Hassidim, and Seth Lloyd. Quantum algorithm for linear systems of equations. *Physical review letters*, 103(15):150502, 2009.
- [10] Andrew M Childs, Robin Kothari, and Rolando D Somma. Quantum algorithm for systems of linear equations with exponentially improved dependence on precision. *SIAM Journal on Computing*, 46(6):1920–1950, 2017.
- [11] Pedro CS Costa, Dong An, Yuval R Sanders, Yuan Su, Ryan Babbush, and Dominic W Berry. Optimal scaling quantum linear-systems solver via discrete adiabatic theorem. *PRX quantum*, 3(4):040303, 2022.
- [12] Di Fang, Lin Lin, and Yu Tong. Time-marching based quantum solvers for time-dependent linear differential equations. *Quantum*, 7:955, 2023.
- [13] Dong An, Jin-Peng Liu, and Lin Lin. Linear combination of Hamiltonian simulation for nonunitary dynamics with optimal state preparation cost. *Physical Review Letters*, 131(15):150603, 2023.
- [14] Dong An, Andrew M Childs, and Lin Lin. Quantum algorithm for linear non-unitary dynamics with near-optimal dependence on all parameters. *Communications in Mathematical Physics*, 407(1):19, 2026.
- [15] Dominic W Berry. High-order quantum algorithm for solving linear differential equations. *Journal of Physics A: Mathematical and Theoretical*, 47(10):105301, 2014.
- [16] Dominic W Berry, Andrew M Childs, Aaron Ostrander, and Guoming Wang. Quantum algorithm for linear differential equations with exponentially improved dependence on precision. *Communications in Mathematical Physics*, 356(3):1057–1081, 2017.
- [17] Mauro ES Morales, Lirandë Pira, Philipp Schleich, Kelvin Koor, Pedro Costa, Dong An, Alán Aspuru-Guzik, Lin Lin, Patrick Rebentrost, and Dominic W Berry. Quantum linear system solvers: A survey of algorithms and applications. *arXiv preprint arXiv:2411.02522*, 2024.
- [18] Roger W Hockney and James W Eastwood. *Computer simulation using particles*. crc Press, 2021.
- [19] Alwyn C Scott. *The nonlinear universe: chaos, emergence, life*. Springer, 2007.
- [20] Fischer Black and Myron Scholes. The pricing of options and corporate liabilities. *Journal of political economy*, 81(3):637–654, 1973.
- [21] Polly Y Yu and Gheorghe Craciun. Mathematical analysis of chemical reaction systems. *Israel Journal of Chemistry*, 58(6-7):733–741, 2018.
- [22] Ilon Joseph. Koopman–von Neumann approach to quantum simulation of nonlinear classical dynamics. *Physical Review Research*, 2(4):043102, 2020.
- [23] Michael Lubasch, Jaewoo Joo, Pierre Moinier, Martin Kiffner, and Dieter Jaksch. Variational quantum algorithms for nonlinear problems. *Physical Review A*, 101(1):010301, 2020.
- [24] Philipp Pfeffer, Florian Heyder, and Jörg Schumacher. Hybrid quantum-classical reservoir computing of thermal convection flow. *Physical review research*, 4(3):033176, 2022.
- [25] Sarah K Leyton and Tobias J Osborne. A quantum algorithm to solve nonlinear differential equations. *arXiv preprint arXiv:0812.4423*, 2008.
- [26] Jin-Peng Liu, Herman Øie Kolden, Hari K. Krovi, Nuno F. Loureiro, Konstantina Trivisa, and Andrew M. Childs. Efficient quantum algorithm for dissipative nonlinear differential equations. *Proceedings of the National Academy of Sciences*, 118(35), 2021.
- [27] David Jennings, Kamil Korzekwa, Matteo Lostaglio, Andrew T. Sornborger, Yigit Subasi, and Guoming Wang. Quantum algorithms for general nonlinear dynamics based on the Carleman embedding. *arXiv: 2509.07155*, 2025.
- [28] Hari Krovi. Improved quantum algorithms for linear and nonlinear differential equations. *Quantum*, 7:913, 2023. Publisher: Verein zur Förderung des Open Access Publizierens in den Quantenwissenschaften.
- [29] Hsuan-Cheng Wu, Jingyao Wang, and Xiantao Li. Quantum algorithms for nonlinear dynamics: Revisiting Carleman linearization with no dissipative conditions. *SIAM Journal on Scientific Computing*, 47(2):A943–A970, 2025.
- [30] Tamás Terlaky and Shuzhong Zhang. Pivot rules for linear programming: a survey on recent theoretical developments. *Annals of operations research*, 46(1):203–233, 1993.
- [31] Dimitris Bertsimas and John N Tsitsiklis. *Introduction to linear optimization*, volume 6. Athena scientific Belmont, MA, 1997.
- [32] Tyler Kharazi, Ahmad M Alkadri, Jin-Peng Liu, Kranthi K Mandadapu, and K Birgitta Whaley. Explicit block encodings of boundary value problems for many-body elliptic operators. *Quantum*, 9:1764, 2025.
- [33] Philipp Schleich, Tyler Kharazi, Xiangyu Li, Jin-Peng Liu, Alán Aspuru-Guzik, and Nathan Wiebe. Arbitrary boundary conditions and constraints in quantum algorithms for differential equations via penalty projections. *arXiv preprint*

arXiv:2506.21751, 2025.

- [34] Amit Surana, Abeynaya Gnanasekaran, and Tuhin Sahai. An efficient quantum algorithm for simulating polynomial dynamical systems. *Quantum Information Processing*, 23(3):105, 2024.
- [35] Judd Katz, Gopikrishnan Muraleedharan, and Abhijeet Alase. Efficient quantum algorithm for solving differential equations with Fourier nonlinearity via Koopman linearization. *arXiv preprint arXiv:2512.06488*, 2025.
- [36] Cheng Xue, Yu-Chun Wu, and Guo-Ping Guo. Quantum homotopy perturbation method for nonlinear dissipative ordinary differential equations. *New Journal of Physics*, 23(12):123035, 2021.
- [37] Seth Lloyd, Giacomo De Palma, Can Gokler, Bobak Kiani, Zi-Wen Liu, Milad Marvian, Felix Tennie, and Tim Palmer. Quantum algorithm for nonlinear differential equations. *arXiv preprint arXiv:2011.06571*, 2020.
- [38] Katsuhiko Endo and Kazuaki Z Takahashi. Divergence-free algorithms for solving nonlinear differential equations on quantum computers. *Physical Review Research*, 8(1):013057, 2026.
- [39] Ivan Novikau and Ilon Joseph. Globalizing the Carleman linear embedding method for nonlinear dynamics. *arXiv preprint arXiv:2510.15715*, 2025.
- [40] David Jennings, Kamil Korzekwa, Matteo Lostaglio, Richard Ashworth, Emanuele Marsili, and Stephen Rolston. An end-to-end quantum algorithm for nonlinear fluid dynamics with bounded quantum advantage. *arXiv preprint arXiv:2512.03758*, 2025.
- [41] Shi Jin, Nana Liu, and Yue Yu. Quantum simulation of partial differential equations via Schrödingerization. *Phys. Rev. Lett.*, 133:230602, 2024.
- [42] Dominic W Berry, Andrew M Childs, and Robin Kothari. Hamiltonian simulation with nearly optimal dependence on all parameters. In *2015 IEEE 56th annual symposium on foundations of computer science*, pages 792–809. IEEE, 2015.
- [43] Dong An, Jin-Peng Liu, Daochen Wang, and Qi Zhao. Quantum differential equation solvers: Limitations and fast-forwarding. *Communications in Mathematical Physics*, 406(8):189, 2025.
- [44] David Jennings, Matteo Lostaglio, Robert B Lowrie, Sam Pallister, and Andrew T Sornborger. The cost of solving linear differential equations on a quantum computer: fast-forwarding to explicit resource counts. *Quantum*, 8:1553, 2024.
- [45] Dong An, Akwum Onwunta, and Gengzhi Yang. Fast-forwarding quantum algorithms for linear dissipative differential equations. *Quantum*, 10:1986, 2026.
- [46] Gengzhi Yang, Akwum Onwunta, and Dong An. Quantum Differential Equation Solvers with Low State Preparation Cost: Eliminating the Time Dependence in Dissipative Equations. *arXiv preprint arXiv:2508.15170*, 2025.
- [47] Xiantao Li and Chunhao Wang. Succinct description and efficient simulation of non-Markovian open quantum systems. *Communications in Mathematical Physics*, 401(1):147–183, 2023.
- [48] Harry Weber and Wolfgang Mathis. Adapting the range of validity for the carleman linearization. *Advances in Radio Science*, 14:51–54, 2016.
- [49] Krzysztof Kowalski and Willi-Hans Steeb. *Nonlinear Dynamical Systems and Carleman Linearization*. World Scientific, 1991.
- [50] <https://github.com/zkjaumich/pivot-shifted-carleman>.
- [51] Elmar Plischke. *Transient effects of linear dynamical systems*. PhD thesis, University of Bremen, 2005.

Appendix A: Oracle construction for the shifted system (Proof of Lemma II.4)

In this section, we provide a more detailed discussion of Lemma II.4. We assume block encoding oracles for the original coefficient matrices F_0, F_1, F_2 with normalization coefficient $\alpha_{F_0}, \alpha_{F_1}, \alpha_{F_2}$, as well as the state preparation oracle for the pivot s . The shifted coefficient matrices follow

$$F_{2,s} = F_2, \quad F_{1,s} = F_1 + F_2(s \otimes I_n + I_n \otimes s), \quad F_{0,s} = F_2 s^{\otimes 2} + F_1 s + F_0. \quad (\text{A1})$$

Then $\alpha_{F_{2,s}} = \alpha_{F_2}$.

Lemma A.1 (block encoding of the tensor product). *Suppose U_A, U_B are the (α_1, a, ϵ) -block encoding of A and (α_2, b, ϵ) -block encoding of B , then there exists $(\alpha_1 \alpha_2, a + b, \epsilon)$ -block encoding of $A \otimes B$ by composing $U_A \otimes U_B$ with $\mathcal{O}(a + b)$ SWAP gates.*

Lemma A.2. (block encoding of the multiplications [7, Proposition 9.12]) *Suppose U_A, U_B are the $(\alpha_1, a, \epsilon_1)$ -block encoding of A and $(\alpha_2, b, \epsilon_2)$ -block encoding of B , then there exists $(\alpha_1 \alpha_2, a + b, \alpha_1 \epsilon_2 + \alpha_2 \epsilon_1 + \epsilon_1 \epsilon_2)$ -block encoding of AB .*

Combined with LCU, we know that I_n is the $(1, 0, 0)$ -block encoding of itself, then there exists the $(2\|s\|, \log(2), 0)$ block encoding of $s \otimes I_n + I_n \otimes s$. Thus, $F_{1,s}$ admits an $(\alpha_{F_1} + 2\|s\|\alpha_{F_2}, a_{F_2} + 2\log(2), (2\|s\| + 1)\epsilon)$ -block encoding. Similarly, $F_{0,s}$ admits an $(\alpha_{F_0} + \alpha_{F_1}\|s\| + \alpha_{F_2}\|s\|^2, a + \log(4), (\|s\|^2 + \|s\| + 1)\epsilon)$ -block encoding.

We also provide detailed discussion to prepare the initial state as the input of the QLSA based quantum algorithm for linear differential equations and shift the final state back to the original differential equation.

a. Preparation of shifted states Finally, we discuss the complexity of preparing shifted states. Given a vector ψ with known norm $\|\psi\|$, and the associated normalized quantum state $|\psi\rangle$, we assume there exists an oracle U_ψ that prepares $|\psi\rangle$ in the form

$$U_\psi |0^{m+1}\rangle = \sqrt{p} |0\rangle |\psi\rangle + \sqrt{1-p} |1\rangle |\Phi\rangle, \quad (\text{A2})$$

where the success probability p is known. By post-selecting the first register on the outcome $|0\rangle$, we obtain the state $|0\rangle |\psi\rangle$. Our goal is to prepare the normalized state associated with the shifted vector $\psi - s$, namely,

$$|\psi - s\rangle := \frac{\psi - s}{\|\psi - s\|},$$

using the oracles O_s and U_ψ . This setting covers both the initial shift and the final shift in Lemma II.4:

- For the initial shift, we take $U_\psi = O_{x(0)}$, and in this case $p = 1$.
- For the final shift, U_ψ is constructed from the QLSA based linear differential equation solvers, we take $U_\psi = U_{u(T)}$, with the corresponding probability p . In this case, we aim to prepare the state $|x(T)\rangle = |u(T) + s\rangle$, which only change the following construction slightly with the same query complexity scaling.

We prepare the state $|\psi - s\rangle$ using one additional ancilla qubit. First, by combining a rotation on the ancilla with controlled- U_ψ , we can prepare

$$\frac{\sqrt{p}\|\psi\|}{\sqrt{\|\psi\|^2 + \|s\|^2}} |0\rangle |0\rangle |\psi\rangle + \frac{\sqrt{p}\|s\|}{\sqrt{\|\psi\|^2 + \|s\|^2}} |1\rangle |0^{m+1}\rangle + \frac{\sqrt{1-p}\|\psi\|}{\sqrt{\|\psi\|^2 + \|s\|^2}} |0\rangle |1\rangle |\Phi\rangle + \frac{\sqrt{1-p}\|s\|}{\sqrt{\|\psi\|^2 + \|s\|^2}} |1\rangle |1\rangle |0^m\rangle.$$

Next, applying controlled- O_s to the last register conditioned on the first ancilla being $|1\rangle$ gives

$$\sqrt{p} \left(\frac{\|\psi\|}{\sqrt{\|\psi\|^2 + \|s\|^2}} |0\rangle |0\rangle |\psi\rangle + \frac{\|s\|}{\sqrt{\|\psi\|^2 + \|s\|^2}} |1\rangle |0\rangle |s\rangle \right) + |\perp\rangle,$$

where $|\perp\rangle$ denotes terms orthogonal to the subspace in which the first two registers are $|0\rangle |0\rangle$ or $|1\rangle |0\rangle$.

Applying a Hadamard gate to the first register yields

$$\frac{\sqrt{p}}{\sqrt{2(\|\psi\|^2 + \|s\|^2)}} |0\rangle |0\rangle (\|\psi\| |\psi\rangle - \|s\| |s\rangle) + |\perp\rangle.$$

Since $\|\psi\| |\psi\rangle = \psi$ and $\|s\| |s\rangle = s$, this becomes

$$\frac{\sqrt{p}\|\psi - s\|}{\sqrt{2(\|\psi\|^2 + \|s\|^2)}} |0\rangle |0\rangle |\psi - s\rangle + |\perp\rangle.$$

Therefore, by amplitude amplification followed by post-selection on the first two registers being $|0\rangle |0\rangle$, we can prepare $|\psi - s\rangle$ using

$$\mathcal{O}\left(\frac{\sqrt{\|\psi\|^2 + \|s\|^2}}{\sqrt{p}\|\psi - s\|}\right)$$

queries to U_ψ , U_ψ^\dagger , O_s , and O_s^\dagger .

Appendix B: Short time convergence for unstable systems

In this section, we provide the proofs for the unstable systems. Throughout the proof we choose $Q = I$ and pivot $s = x(0)$, it reveals that $v(0) = 0$ and $E_{i,s} = F_{i,s}$ for all $i = 0, 1, 2$. The error from the algorithm are mainly from Carleman truncation error and the error from the QLSA based quantum algorithm for linear differential equations.

1. Convergence of the Carleman linearization

We first prove Proposition IV.4 using the following bound for the solution $v(t)$.

Lemma B.1 (General system: short time bound of $\|v(t)\|$). *Consider $v(t)$ satisfying Eq. (22). Let $Q = I$ and choose the pivot $s = x(0)$. Then $v(0) = 0$. Moreover, there exists $t' > 0$ such that*

$$\|v(t)\| \leq 1, t \leq T \leq t'. \quad (\text{B1})$$

In particular, one may choose

$$t' = \frac{1}{\|F_{2,s}\| + \|F_{1,s}\| + \|F_{0,s}\|}, \quad (\text{B2})$$

then for all $t < t'$,

$$\|v(t)\| \leq t(\|F_{2,s}\| + \|F_{1,s}\| + \|F_{0,s}\|) < 1. \quad (\text{B3})$$

With Lemma B.1, the norm of the solution can be bounded by one for any time $t < t'$. With this short time bound of $\|v(t)\|$, we can prove the convergence of Carleman truncation accordingly.

Proof of Proposition IV.4. The error vector $\xi(t)$ satisfies the differential equation in Eq. (35),

$$\partial_t \xi = B_N \xi + \hat{d}_N, \xi(0) = 0 \quad (\text{B4})$$

i.e., the error vector can be written using the integral

$$\xi(t) = \int_0^t e^{B_N(t-\tau)} \hat{d}_N(\tau) d\tau. \quad (\text{B5})$$

Let $C(B_N) = \sup_{t \in [0, T]} \|e^{B_N t}\|$ and $\Lambda = \sum_{j=1}^N |j\rangle\langle j| \otimes 1/j$. Notice that by [51, Theorem 3.35], we have $\|e^{B_N t}\| \leq \sqrt{\kappa_\Lambda} e^{\mu_\Lambda(B_N)t}$. Additionally, similar to the proof in Eq. (42), we replace B_N with ΛB_N , then

$$\begin{aligned} & \xi^\dagger (\Lambda B_N + B_N^\dagger \Lambda) \xi \\ &= \sum_j \frac{1}{j} \xi_j^\dagger (B_{j,j} + B_{j,j}^\dagger) \xi_j + \sum_j \xi_{j+1}^\dagger \left(\frac{1}{j+1} B_{j+1,j} + \frac{1}{j+1} B_{j,j+1}^\dagger \right) \xi_j + \sum_j \xi_j^\dagger \left(\frac{1}{j} B_{j+1,j}^\dagger + \frac{1}{j} B_{j,j+1} \right) \xi_{j+1} \\ &\leq \sum_j \frac{2}{j} \mu(B_{j,j}) \|\xi_j\|^2 + \sum_j \frac{2}{j+1} \|B_{j+1,j}\| \|\xi_j\| \|\xi_{j+1}\| + \sum_j \frac{2}{j} \|B_{j,j+1}\| \|\xi_j\| \|\xi_{j+1}\| \\ &\leq \sum_j 2\mu(F_{1,s}) \|\xi_j\|^2 + 2\|F_{0,s}\| \|\xi_j\| \|\xi_{j-1}\| + 2\|F_{2,s}\| \|\xi_j\| \|\xi_{j-1}\| \\ &\leq \xi_{\tilde{G}}^\dagger (\tilde{G} + \tilde{G}^\dagger) \xi_{\tilde{G}} \leq 2\mu(\tilde{G}) \|\xi_{\tilde{G}}\|^2, \end{aligned} \quad (\text{B6})$$

where $\tilde{G} \in \mathbb{C}^{N \times N}$:

$$\tilde{G}_{j,j} = \mu(F_{1,s}), \tilde{G}_{j-1,j} = \|F_{0,s}\|, \tilde{G}_{j+1,j} = \|F_{2,s}\|. \quad (\text{B7})$$

Then by Gershgorin circle theorem,

$$\mu(\Lambda B_N + B_N^\dagger \Lambda) \leq \mu(F_{1,s}) + \|F_{0,s}\| + \|F_{2,s}\|. \quad (\text{B8})$$

The log norm becomes

$$\begin{aligned} \mu_\Lambda(B_N) &= -\frac{1}{2} \min_{x \neq 0} \frac{\langle x, (\Lambda B_N + B_N^\dagger \Lambda) x \rangle}{\langle x, \Lambda x \rangle} = \frac{1}{2} \lambda_{\max} \left(\Lambda^{-1/2} (\Lambda B_N + B_N^\dagger \Lambda) \Lambda^{-1/2} \right) \\ &\leq \frac{\|\Lambda^{-1/2}\|^2}{2} (\mu(F_{1,s}) + \|F_{0,s}\| + \|F_{2,s}\|) \leq \frac{N}{2} (\mu(F_{1,s}) + \|F_{0,s}\| + \|F_{2,s}\|) \end{aligned} \quad (\text{B9})$$

by [51, Lemma 3.31]. Then we have

$$C(B_N) \leq \sqrt{N} \sup_{t \in [0, T]} e^{\frac{N}{2}(\mu(F_{1,s}) + \|F_{0,s}\| + \|F_{2,s}\|)t}. \quad (\text{B10})$$

From Lemma B.1, let $t' = \frac{1}{\|F_{2,s}\| + \|F_{1,s}\| + \|F_{0,s}\|}$ then $\|v(t)\| \leq 1$ for all $t < t'$. For any $t \leq t'$, the Carleman truncation error ξ can be bounded as

$$\begin{aligned} \|\xi(t)\| &\leq tC(B_N) \sup_{t \in [0, T]} \|\hat{d}_N(t)\| \\ &\leq t\sqrt{N} \sup_{\tau \in [0, t]} e^{\frac{N}{2}(\mu(F_{1,s}) + \|F_{0,s}\| + \|F_{2,s}\|)t} \|B_{N, N+1}\| \sup_{\tau \in [0, t]} \|v(\tau)\|^{N+1} \\ &\leq tN^{3/2} \|F_{2,s}\| \left(t(\|F_{2,s}\| + \|F_{1,s}\| + \|F_{0,s}\|) e^{\frac{1}{2}(\mu(F_{1,s}) + \|F_{0,s}\| + \|F_{2,s}\|)t} \right)^N, \end{aligned} \quad (\text{B11})$$

where we use the fact that $\|B_{N, N+1}\| \leq N\|F_{2,s}\|$ and the short time bound of $\|v(t)\|$ in Lemma B.1.

Set $t^* < t'/e$ so that

$$t^* (\|F_{2,s}\| + \|F_{1,s}\| + \|F_{0,s}\|) e^{\frac{1}{2}(\mu(F_{1,s}) + \|F_{0,s}\| + \|F_{2,s}\|)t^*} \leq t^* (\|F_{2,s}\| + \|F_{1,s}\| + \|F_{0,s}\|) e < 1.$$

For all $t \leq t^*$, the Carleman error $\xi(t)$ decays exponentially with respect to the truncation order N . In particular, for any $T \in [0, t^*]$, the Carleman error can be bounded as $\|\xi(T)\| \leq \epsilon \|v(T)\|$ by choosing the truncation order

$$N \geq \Theta \left(\frac{\log(T\|F_{2,s}\| / (\|v(T)\|\epsilon))}{\log(1 / (t^* (\|F_{2,s}\| + \|F_{1,s}\| + \|F_{0,s}\|) e))} \right).$$

This completes the proof of Proposition IV.4. □

The details in proving the short time bound on the norm of $v(t)$ are provided as follows.

Proof of Lemma B.1. Since $\|v(0)\| = 0$, there exists a short time interval so that $\|v(t)\| \leq 1$. From

$$\partial_t v = F_{2,s} v^{\otimes 2} + F_{1,s} v + F_{0,s}, \quad (\text{B12})$$

we have the integral form as

$$v(t) = \int_0^t F_{2,s} v^{\otimes 2}(\tau) + F_{1,s} v(\tau) + F_{0,s} d\tau \quad (\text{B13})$$

Then the bound for the norm

$$\|v(t)\| \leq \int_0^t \|F_{2,s}\| \|v(\tau)\|^2 + \|F_{1,s}\| \|v(\tau)\| + \|F_{0,s}\| d\tau \leq \int_0^t (\|F_{2,s}\| + \|F_{1,s}\| + \|F_{0,s}\|) d\tau = t(\|F_{2,s}\| + \|F_{1,s}\| + \|F_{0,s}\|). \quad (\text{B14})$$

We may choose

$$t' = \frac{1}{\|F_{2,s}\| + \|F_{1,s}\| + \|F_{0,s}\|}, \quad (\text{B15})$$

then for all $t < t'$,

$$\|v(t)\|^2 < 1. \quad (\text{B16})$$

□

2. Quantum solvers for linear differential equations

Next, we incorporate the error from the QLSA based quantum solver for linear differential equations with the corresponding query complexity.

Proof of Proposition IV.8. The complexity for differential systems remains unstable after pivot shift can be obtained by applying the quantum solver for linear differential equations in [28] where we still use truncated Taylor series to approximate the solution of linear differential equations while constructing the linear system in a slightly different way in Eq. (29).

Lemma B.2. ([28, Theorem 7]) *For any sparse matrix A with sparsity s , dimension d and $C(A) = \max_{t \in [0, T]} \|e^{At}\|$. Using the truncated Taylor series methods to solve linear differential equation $\partial_t u = Au + b$. Let $\epsilon > 0$ be the target error then we can obtain an ϵ -approximation of the final state $u(T)/\|u(T)\|$ using*

$$\mathcal{O} \left(g_u T \|A\| C(A) \text{poly} \left(s, \log(n), \log \left(1 + \frac{Te^2 \|b\|}{\|x(T)\|} \right), \log \left(\frac{1}{\epsilon} \right), \log(T \|A\| C(A)) \right) \right) \quad (\text{B17})$$

queries to the oracles O_A , O_b and $O_{u(0)}$. Here $C(A) = \max_{t \in [0, T]} \|e^{At}\|$ and $g_u = \frac{\max_{t \in [0, T]} \|u(t)\|}{\|u(T)\|}$.

Follow the same idea in the proof of Proposition IV.7, we first apply the lemma to solve the Carleman linearized equation $\partial_t \hat{z} = B_N \hat{z} + d_N$, and quantify the extra cost from amplitude amplification by obtaining the approximation of the state $|u(T)\rangle$. We note that, when $s = x(0)$, we have $v(0) = \vec{0}$ and the initial state preparation is not necessary.

We denote the quantum state after applying the above algorithm as $|\tilde{z}\rangle$. It approximates solution of the linearized differential equation at the end time $\hat{z}(T)$ up to precision ϵ' . From Lemma B.2, there exists a quantum algorithm that output the state $|\tilde{z}\rangle$ such that

$$\left\| \tilde{z} - \frac{\hat{z}(T)}{\|\hat{z}(T)\|} \right\| \leq \epsilon' \quad (\text{B18})$$

with

$$\mathcal{O} \left(g_{\tilde{z}} T \|B_N\| C(B_N) \text{poly} \left(C_s, \log(\dim(B_N)), \log \left(1 + \frac{Te^2 \|d_N\|}{\|\hat{z}(T)\|} \right), \log \left(\frac{1}{\epsilon'} \right), \log(T \|B_N\| C(B_N)) \right) \right) \quad (\text{B19})$$

queries to oracles for $B_N, |d_N\rangle$. Here C_s is the sparsity of the matrix B_N .

From Proposition IV.4, the relative error from Carleman truncation can be bounded by δ' , $\|\xi(T)\| \leq \delta' \|v(T)\|$ by choosing

$$N \geq \Theta \left(\frac{\log(T \|F_{2,s}\| / (\|v(T)\| \epsilon))}{\log(1 / (t^* (\|F_{2,s}\| + \mu(F_{1,s}) + \|F_{0,s}\|) e))} \right). \quad (\text{B20})$$

where $t^* < \frac{1}{e(\|F_{2,s}\| + \|F_{1,s}\| + \|F_{0,s}\|)}$.

By measuring the registers, we extract the first block $|\tilde{z}_1\rangle$ of the quantum state output from the QLSA algorithm and use it to approximate $|u(T)\rangle$. This block has the same dimension as the solution when the Carleman truncation order $N = 1$. Follow the same approximation in Eqs. (69) to (71), we choose $\epsilon' = \Theta\left(\frac{\epsilon}{\sqrt{N}}\right)$, $\delta' = \Theta(\epsilon)$, so that $\|\tilde{z}_1\| \geq \Theta(1/\sqrt{N})$ and $\left\| \frac{|\tilde{z}_1\rangle}{\|\tilde{z}_1\|} - \frac{v(T)}{\|v(T)\|} \right\| \leq \mathcal{O}(\epsilon)$. The success probability can be boosted to a constant by $\mathcal{O}(\sqrt{N})$ rounds of amplitude amplification.

Furthermore, the parameters in the query complexity can be approximated explicitly as

- The norm of B_N can be bounded as $\|B_N\| = \mathcal{O}(N(\alpha_{F_{0,s}} + \alpha_{F_{1,s}} + \alpha_{F_{2,s}}))$.
- The sparsity of matrix B_N , $C_s \leq 3Nn^2$.
- The dimension of B_N , $\frac{n^{N+1}-1}{n-1}$.
- From the proof of Proposition IV.4,

$$C(B_N) = \sup_{t \in [0, T]} \|e^{B_N t}\| \leq \sqrt{N} \sup_{t \in [0, T]} e^{\frac{N}{2}(\mu(F_{1,s}) + \|F_{0,s}\| + \|F_{2,s}\|)t} \leq \sqrt{N} e^N,$$

- The solution ratio coefficient

$$g_{\tilde{z}} = \frac{\max_{t \in [0, T]} \|\hat{z}(t)\|}{\|\hat{z}(T)\|} \leq \sqrt{N} \frac{1 + \delta'}{1 - \delta'} \frac{\max_{t \in [0, T]} \|v(t)\|}{\|v(T)\|} = \sqrt{N} \frac{1 + \delta'}{1 - \delta'} g_v, \quad (\text{B21})$$

with $g_v = \frac{\max_{t \in [0, T]} \|v(t)\|}{\|v(T)\|}$.

- $\|\hat{z}(T)\| \geq \|v(T)\|(1 - \delta')$.

Combining the complexity from the quantum algorithm with the amplitude amplification overhead, we have an ϵ -approximation of $|v(T)\rangle = |u(T)\rangle$ using

$$\begin{aligned}
& \mathcal{O} \left(\underbrace{g_z T \|B_N\| C(B_N) \text{ poly} \left(C_s, \log(\dim(B_N)), \log \left(1 + \frac{T e^2 \|d_N\|}{\|\hat{z}(T)\|} \right), \log \left(\frac{1}{\epsilon'} \right), \log(T \|B_N\| C(B_N)) \right)}_{\text{From Eq. (B19)}} \times \underbrace{\sqrt{N}}_{\text{Amplitude Amplification}} \right) \\
&= \mathcal{O} \left(g_v N^2 (\alpha_{F_{0,s}} + \alpha_{F_{1,s}} + \alpha_{F_{2,s}}) T e^N \text{ poly} \left(C_s, \log \left(\frac{n^{N+1} - 1}{n - 1} \right), \log \left(1 + \frac{T e^2 \|d_N\|}{\|\hat{z}(T)\|} \right), \log \left(\frac{1}{\epsilon'} \right), \log(T \|B_N\| C(B_N)) \right) \right) \\
&= \mathcal{O} \left(g_v \text{ poly}(N) T^2 \frac{(\alpha_{F_{0,s}} + \alpha_{F_{1,s}} + \alpha_{F_{2,s}}) \|F_{2,s}\|}{\|v(T)\| \delta'} \text{ poly} \left(C_s, \log(n), \log \left(1 + \frac{T e^2 \|F_{0,s}\|}{\|v(T)\|} \right), \log \left(\frac{\sqrt{N}}{\epsilon} \right), \log(T \|B_N\| C(B_N)) \right) \right) \\
&= \tilde{\mathcal{O}} \left(g_v \frac{(\alpha_{F_{0,s}} + \alpha_{F_{1,s}} + \alpha_{F_{2,s}}) \|F_{2,s}\| T^2}{\|v(T)\| \epsilon} \text{ polylog}(n) \right)
\end{aligned} \tag{B22}$$

queries to the oracle for B_N , $|d_N\rangle$.

In summary, the algorithm requires

$$\tilde{\mathcal{O}} \left(g_v \frac{(\alpha_{F_{0,s}} + \alpha_{F_{1,s}} + \alpha_{F_{2,s}}) \|F_{2,s}\| T^2}{\|v(T)\| \epsilon} \text{ polylog}(n) \right) \tag{B23}$$

queries to the block encoding for $F_{i,s}$. □

Proof of Theorem IV.2. The proof of this theorem is very similar to the proof of Theorem IV.1. The only difference is that we don't need to consider the transfer between u and v and prepare $|v(0)\rangle$ since $Q = I$ and $s = x(0)$.

The last step of the algorithm requires $\mathcal{O} \left(\frac{\sqrt{\|x(T) - s\|^2 + \|s\|^2}}{\|x(T)\|} \right)$ queries to the oracles for $|u(T)\rangle$ and $|s\rangle = |x(0)\rangle$ to prepare the final state $|x(T)\rangle$.

Consequently, there exists a quantum algorithm that outputs the ϵ -approximation of the state $|x(T)\rangle$ using

$$\tilde{\mathcal{O}} \left(\underbrace{\frac{\sqrt{\|x(T) - s\|^2 + \|s\|^2}}{\|x(T)\|}}_{\text{Final state shift}} g_v \frac{(\alpha_{F_{0,s}} + \alpha_{F_{1,s}} + \alpha_{F_{2,s}}) \|F_{2,s}\| T^2}{\|v(T)\| \epsilon} \text{ polylog}(n) \right) \tag{B24}$$

queries to the block-encoding of $F_{i,s}$. Here, $\alpha_{F_{i,s}}$ is the block-encoding factor for $F_{i,s}$, defined in Lemma II.4.

Plugging $\alpha_{F_{2,s}} = \alpha_{F_2}$, $\alpha_{F_{1,s}} = \alpha_{F_1} + 2\|s\|\alpha_{F_2}$ and $\alpha_{F_{0,s}} = \alpha_{F_0} + \alpha_{F_1}\|s\| + \alpha_{F_2}\|s\|^2$, $\|F_{2,s}\| = \|F_2\|$, and $s = x(0)$, the query complexity becomes

$$\tilde{\mathcal{O}} \left(\frac{\sqrt{\|x(T) - x(0)\|^2 + \|x(0)\|^2}}{\|x(T)\|} \frac{(\alpha_{F_0} + \alpha_{F_1} + \alpha_{F_2}) (1 + \|x(0)\|)^2 \|F_2\| T^2 g_v}{\|x(T) - x(0)\| \epsilon} \text{ polylog}(n) \right), \tag{B25}$$

to oracles for F_i and $|x(0)\rangle$, we complete the proof. □

Appendix C: Comparison with the pivot-switching method of [38]

The pivot-switching (PS) method of [38] differs from our pivot-shifted construction in two key respects. First, in [38] the pivot s is updated dynamically along the trajectory, whereas the present work uses a single, fixed pivot. Second, the lifted state in [38] is built from the original variable x rather than the shifted variable u :

$$\hat{z}_{\text{PS}} = [x; x^{\otimes 2}; \dots; x^{\otimes N}]^\top. \tag{C1}$$

Pivot switching can be viewed as a sequence of pivot shifts. Here, we only focus on a single pivot shift, corresponding to one step of pivot switching.

We start from the shifted quadratic representation, as in our PSC method,

$$\partial_t u = F_{2,s} u^{\otimes 2} + F_{1,s} u + F_{0,s}, \quad u = x - s. \quad (\text{C2})$$

Equivalently, in the x variable,

$$\partial_t x = \tilde{F}_{2,s} x^{\otimes 2} + \tilde{F}_{1,s} x + \tilde{F}_{0,s}, \quad (\text{C3})$$

where

$$\begin{aligned} \tilde{F}_{2,s} &= F_{2,s}, \\ \tilde{F}_{1,s} &= F_{1,s} - F_{2,s} (I \otimes s + s \otimes I), \\ \tilde{F}_{0,s} &= F_{0,s} - F_{1,s} s + F_{2,s} s^{\otimes 2}. \end{aligned} \quad (\text{C4})$$

For $j < N$, no truncation is applied because

$$\frac{d}{dt} x^{\otimes j}$$

contains powers no higher than $x^{\otimes(j+1)}$, which is still included in the order- N lifted state. Thus the first $N - 1$ block rows of the PS matrix have the same quadratic Carleman form in the x basis:

$$\begin{aligned} (B_{\text{PS}}^{(N)})_{j,j+1} &= \tilde{F}_{2,s} \otimes I^{\otimes(j-1)} + I \otimes \tilde{F}_{2,s} \otimes I^{\otimes(j-2)} + \dots + I^{\otimes(j-1)} \otimes \tilde{F}_{2,s}, \\ (B_{\text{PS}}^{(N)})_{j,j} &= \tilde{F}_{1,s} \otimes I^{\otimes(j-1)} + I \otimes \tilde{F}_{1,s} \otimes I^{\otimes(j-2)} + \dots + I^{\otimes(j-1)} \otimes \tilde{F}_{1,s}, \\ (B_{\text{PS}}^{(N)})_{j,j-1} &= \tilde{F}_{0,s} \otimes I^{\otimes(j-1)} + I \otimes \tilde{F}_{0,s} \otimes I^{\otimes(j-2)} + \dots + I^{\otimes(j-1)} \otimes \tilde{F}_{0,s}, \end{aligned} \quad (\text{C5})$$

for $1 \leq j < N$.

The only structural difference appears in the last block row. Before truncation, the last lifted equation contains

$$(B_{\text{PS}}^{(N)})_{N,N+1} x^{\otimes(N+1)}. \quad (\text{C6})$$

However, the PS method truncates in the shifted variable $u = x - s$, so the order $N + 1$ term in u is removed. Equivalently,

$$x^{\otimes(N+1)} \longmapsto x^{\otimes(N+1)} - (x - s)^{\otimes(N+1)}. \quad (\text{C7})$$

Since

$$(x - s)^{\otimes(N+1)} = x^{\otimes(N+1)} + \sum_{k=0}^N R_{N+1,k}(-s) x^{\otimes k}, \quad (\text{C8})$$

the highest-order term cancels and only lower-order terms remain:

$$x^{\otimes(N+1)} - (x - s)^{\otimes(N+1)} = - \sum_{k=0}^N R_{N+1,k}(-s) x^{\otimes k}. \quad (\text{C9})$$

Here $R_{N+1,k}(-s)$ denotes the coefficient matrix of $x^{\otimes k}$ in the expansion of $(x - s)^{\otimes(N+1)}$.

Therefore, the PS matrix has the schematic form

$$B_{\text{PS}}^{(N)} = \begin{bmatrix} B_{1,1}^x & B_{1,2}^x & 0 & \cdots & 0 \\ B_{2,1}^x & B_{2,2}^x & B_{2,3}^x & \ddots & \vdots \\ 0 & B_{3,2}^x & B_{3,3}^x & \ddots & 0 \\ \vdots & \ddots & \ddots & \ddots & B_{N-1,N}^x \\ C_1 & C_2 & C_3 & \cdots & C_N \end{bmatrix}, \quad (\text{C10})$$

where the first $N - 1$ rows are block tridiagonal, while the last row is dense. The dense last-row blocks are

$$C_k = \delta_{k,N-1} B_{N,N-1}^x + \delta_{k,N} B_{N,N}^x - B_{N,N+1}^x R_{N+1,k}(-s), \quad 1 \leq k \leq N. \quad (\text{C11})$$

The corresponding affine term is

$$d_{\text{PS}}^{(N)} = \begin{bmatrix} \tilde{F}_{0,s} \\ 0 \\ \vdots \\ -B_{N,N+1}^x R_{N+1,0}(-s) \end{bmatrix}. \quad (\text{C12})$$

Moreover, PSC and PS are equivalent up to a change of coordinates. Indeed, the two lifted states are related by the finite translation map induced by $x = u + s$:

$$\hat{z}_{\text{PS}} = T_N(s) \hat{z}_{\text{PSC}}, \quad (\text{C13})$$

where $T_N(s)$ expands each tensor power

$$x^{\otimes j} = (u + s)^{\otimes j}, \quad 1 \leq j \leq N. \quad (\text{C14})$$

The inverse map is obtained by replacing s with $-s$, since $u = x - s$:

$$\hat{z}_{\text{PSC}} = T_N(-s) \hat{z}_{\text{PS}}, \quad T_N(s)^{-1} = T_N(-s). \quad (\text{C15})$$

Therefore, if the PSC system is written as

$$\frac{d}{dt} \hat{z}_{\text{PSC}} = B_{\text{PSC}}^{(N)} \hat{z}_{\text{PSC}} + d_{\text{PSC}}^{(N)}, \quad (\text{C16})$$

then the same truncated dynamics expressed in the x basis is

$$\frac{d}{dt} \hat{z}_{\text{PS}} = T_N(s) B_{\text{PSC}}^{(N)} T_N(-s) \hat{z}_{\text{PS}} + T_N(s) d_{\text{PSC}}^{(N)}. \quad (\text{C17})$$

Thus,

$$B_{\text{PS}}^{(N)} = T_N(s) B_{\text{PSC}}^{(N)} T_N(-s), \quad d_{\text{PS}}^{(N)} = T_N(s) d_{\text{PSC}}^{(N)}. \quad (\text{C18})$$

This shows that the PS method does not define a different truncated trajectory. It rewrites the same shifted-order truncation in the unshifted x -coordinates. Consequently, when the lifted initial conditions are chosen consistently,

$$\hat{z}_{\text{PS}}(0) = T_N(s) \hat{z}_{\text{PSC}}(0), \quad (\text{C19})$$

the two methods satisfy

$$\hat{z}_{\text{PS}}(t) = T_N(s) \hat{z}_{\text{PSC}}(t), \quad (\text{C20})$$

and therefore recover the same physical solution $x(t) = u(t) + s$.

The practical difference is not the approximation itself, but the matrix representation: PSC remains sparse and block tridiagonal, whereas the PS construction generally produces a dense final block row after the coordinate transformation, which is inefficient for block encoding and quantum simulation. This dense row comes precisely from re-expressing the removed shifted term $u^{\otimes(N+1)}$ in the unshifted x basis.